

See discussions, stats, and author profiles for this publication at: <https://www.researchgate.net/publication/268332687>

Detrital zircon geochronology in blueschist-facies meta-conglomerates from the Western Alps: implications for the late Carboniferous to early Permian palaeogeography

ARTICLE *in* INTERNATIONAL JOURNAL OF EARTH SCIENCES · APRIL 2015

Impact Factor: 2.09 · DOI: 10.1007/s00531-014-1104-8

CITATION

1

READS

63

3 AUTHORS:



Paola Manzotti

University of Lausanne

23 PUBLICATIONS 67 CITATIONS

[SEE PROFILE](#)



Marc Poujol

Université de Rennes 1

131 PUBLICATIONS 979 CITATIONS

[SEE PROFILE](#)



Michel Ballèvre

Université de Rennes 1

114 PUBLICATIONS 1,869 CITATIONS

[SEE PROFILE](#)

Detrital zircon geochronology in blueschist-facies meta-conglomerates from the Western Alps: implications for the late Carboniferous to early Permian palaeogeography

Paola Manzotti · Marc Poujol · Michel Ballèvre

Received: 29 April 2014 / Accepted: 1 November 2014
© Springer-Verlag Berlin Heidelberg 2014

Abstract In the Western Alps, the Money Complex of the Gran Paradiso Massif, metamorphosed under blueschist facies during the Alpine cycle, is considered to be Permo-Carboniferous in age, but no palaeontological or radiometric data constrain this interpretation. A revision of the lithostratigraphy of the Money Complex allows recognizing a polygenic (graphite-rich) and a monogenic (graphite-poor) meta-sedimentary formation. Detrital zircon U–Pb geochronology in both meta-sedimentary formations shows that (i) the main population is Cambrian and Ordovician in age, (ii) the youngest grains are Silurian and Lower Devonian, and (iii) Carboniferous zircon grains are lacking. A careful study of the age distributions in the Alps suggests that potential source for the detrital material in the Money Complex is the Briançonnais basement. Late Carboniferous magmatism is widespread in the Helvetic Zone of the Alps. Permian magmatism is dominant in the Briançonnais, the Austroalpine and the Southalpine basements. The lack of Carboniferous zircons in the Money Complex suggests that the detritus was not shed from the Helvetic zone, which was separated from the Money basin by the Zone Houillère basin, where the main drainage pattern was developed from south to north and where the depocenters migrated northwards from the Upper Mississippian to Upper Pennsylvanian. We suggest that the Money Complex may have been located to the east of the main river drainage inside the

Zone Houillère basin or alternatively may represent a small basin, located on the east of the Zone Houillère.

Keywords Money Unit · Gran Paradiso · Permo-Carboniferous evolution · Detrital zircon

Introduction

The late Palaeozoic history of southern Europe is characterized by three main geodynamic events: (i) the convergence between major plates (Gondwana and Eurasia) leading to the Variscan orogeny (Devonian-early to late Carboniferous), (ii) a drastic change in the plate kinematics (late Carboniferous-early Permian) resulting in the transformation of the Gondwana-Eurasia collisional margin into a diffuse dextral transform margin, recorded by the orogenic collapse, and (iii) the opening of the Neotethys Ocean during the Middle-Upper Permian, recorded by the progressive westward marine ingression (von Raumer 1998; Cassinis et al. 2012; von Raumer 2013). This evolution was also marked by a progressive change in the climate, which became drier across Europe (Kutzbach and Ziegler 1993; Schönlaub 1993; Schneider et al. 2006). The records of these geodynamic events and of this climate change are preserved in detrital sediments, at present located in different sectors of the Western and Central Alps (Fig. 1; Supplementary data Table 1).

In the External Zone (External Massifs and Helvetic nappes) of the Alpine belt, numerous Carboniferous basins of small sizes occur, such as the La Mure basin in the Belledonne Massif (Gignoux and Moret 1952) and the Salvan-Dorenaz basin in the Aiguilles Rouges Massif (Niklaus and Wetzel 1996; Brousmiche Delcambre et al. 1999). In the frontal part of the Briançonnais domain, the

Electronic supplementary material The online version of this article (doi:10.1007/s00531-014-1104-8) contains supplementary material, which is available to authorized users.

P. Manzotti (✉) · M. Poujol · M. Ballèvre
Géosciences Rennes, UMR-CNRS 6118, Université de Rennes 1,
Campus de Beaulieu, 35042 Rennes Cedex, France
e-mail: paola.manzotti@univ-rennes1.fr

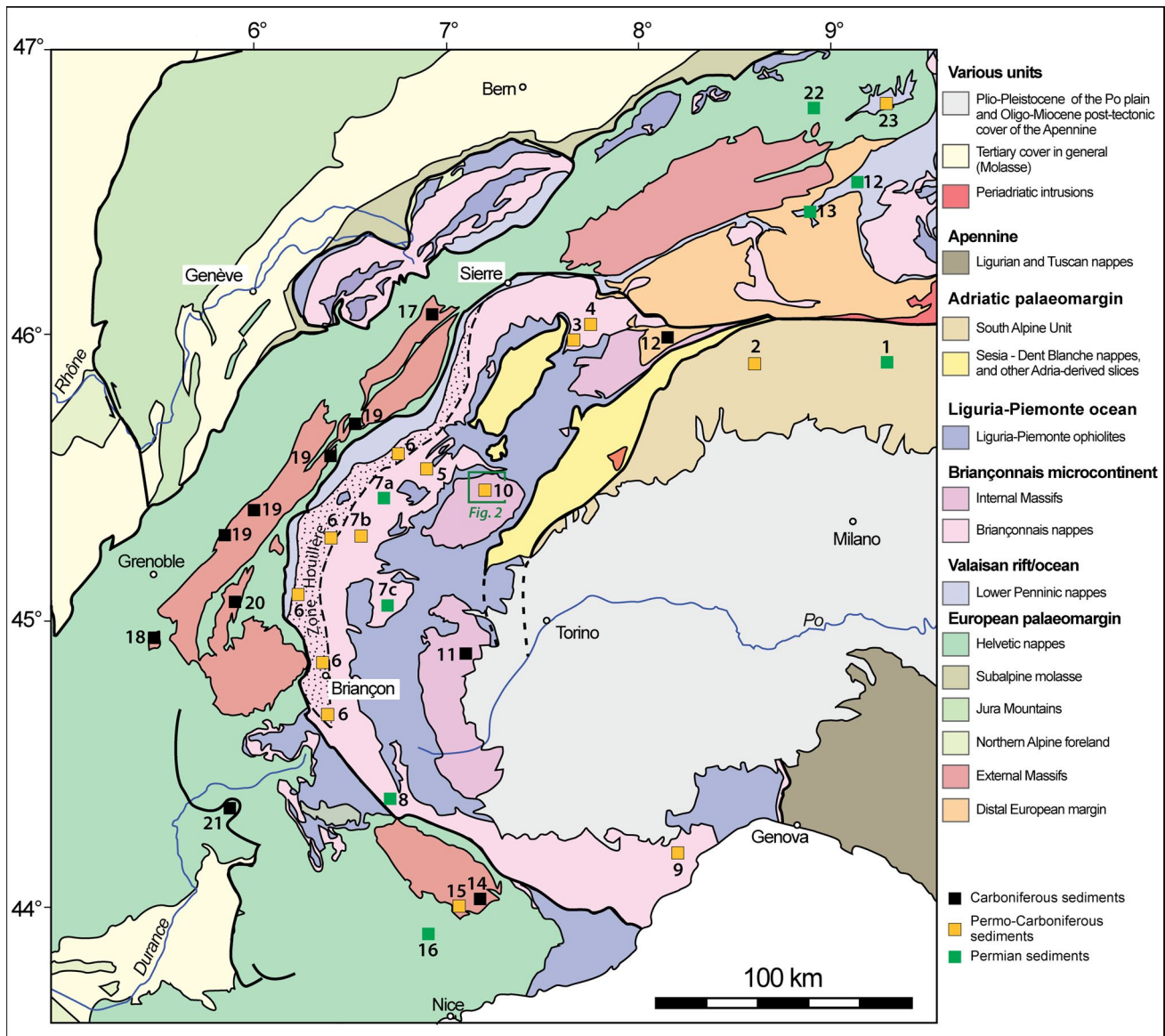


Fig. 1 a The Money Unit (square no 10) of the Gran Paradiso Massif in the Western Alps: simplified structural and geological map (modified after Schmid et al. 2004). Location of the Carboniferous, Permo-Carboniferous, and Permian deposits is represented by black, orange, and green squares, respectively. 1 Ponteranica Conglomerate; 2 Basal Conglomerate; 3 Distulberg, Bruneggjoch and Chassoure Formations; 4 Törbel and Moosalp Formations; 5 Grand Saint Bernard nappe (Valsavarenche and Rhêmes valleys); 6 Zone Houillère; 7a Northern Vanoise; 7b Southern Vanoise; 7c Ambin Massif; 8 Zona di Acceglie

Zone Houillère exposes Carboniferous graphite-bearing detrital sequences over 100 km from south to north. Other occurrences of graphite-bearing detrital sequences, classically assumed to be Carboniferous in age, are now exposed as tectonic windows below the eclogite-facies units of the Internal Massifs (Novarese 1894, 1895, 1896; Vialon 1966; Compagnoni et al. 1974). Carboniferous sequences are not frequently found in the Southalpine unit, whereas Permian

(Combrémont and Maniglia Series); 9 Briançonnais Ligure (Ollano and Verrucano Formations); 10 Money Unit; 11 Pinerolo Unit; 12 Salarioli Unit (Ruginenta); 13 Luzzzone-Terri nappe; 14 Synclinal de Férisson-Montjoya and Synclinal de Las Crotas; 15 Saint-Sauver Series; 16 Barrot Unit; 17 Salvan-Dorénaz; 18 La Mure; 19 Belledonne; 20 Massif des Grandes Rousses; and 21 Clue de Verdaches-Barles. See supplementary data Table 1 for a detailed description of the main characters, ages, and references of the sedimentary deposits reported in Fig. 1

continental basins (e.g. the Orobic and Collio basins) are well developed (Cassinis et al. 2012). In the External Zone (External Massifs and Helvetic nappes) of the Alpine belt and in the Southalpine unit, where the Alpine deformation has been less intense, the detrital sequences frequently rest on a metamorphic basement and the faults that bound the basins are still recognizable (Capuzzo and Wetzel 2004; Cassinis and Perotti 2007).

All the Carboniferous to Permian continental deposits, now located in the Alpine region, contain fluvio-lacustrine sediments as well as volcanics of calc-alkaline affinity, acidic-to-intermediate in composition. In the Alps, the ages of the Carboniferous to Permian sedimentary sequences have been mostly established on the basis of biostratigraphy (Portis 1887; Corsin and Faure-Muret 1946; Venzo and Maglia 1947; Ellenberger 1958; Jongmans 1960; Greber 1965; Schade et al. 1985; Brousmiche Delcambre et al. 1999). The palaeontological record of these sedimentary sequences mainly consists of macro- and microflora, palynomorphs, and tetrapod footprints (e.g. Greber 1965; Cassinis and Doubinger 1992; Nicosia et al. 2000; Ronchi et al. 2012). Only in some cases, radiometric investigations (Capuzzo and Bussy 2000; Cassinis et al. 2002 and refs therein) have been performed on intrusive and extrusive rocks located within these basins (Supplementary data Table 1).

In the lack of biostratigraphic constraints, detrital zircon U–Pb geochronology is a powerful tool to provide a maximum age for sedimentation (Lahtinen et al. 2002; Fedo et al. 2003; Kebede et al. 2005; Malusà et al. 2013). Precise temporal constraints can be provided, because zircon grains are chemically stable during weathering and mechanically durable during transport towards the depositional environments. Thanks to their resilient nature, detrital zircons are commonly found in continental clastic sediments. They derive from the erosion of basement rocks as well as of syn-depositional or closely contemporaneous volcanic rocks, located either within or even outside of the basin. Detrital zircon U–Pb geochronology has been largely used in sedimentary sequences in several terranes (e.g. Decelles et al. 2004; Teipel et al. 2004; Darby and Gehrels 2006; Hietpas et al. 2011; Thern and Nelson 2012; Ducassou et al. 2014; Kydonakis et al. 2014) with the aim to (i) provide a maximum age for sedimentation, (ii) discuss the provenance of the detrital materials, and (iii) support palaeogeographical reconstitutions. In the Alps, this approach has been successfully employed to assess the sediment provenances on modern and ancient (unmetamorphosed) sedimentary successions (Malusà et al. 2011, 2013). Detrital geochronology has been applied to meta-sedimentary sequences in only one case, in the Eastern Alps (Kebede et al. 2005). This work aims to study the Money Complex in the Western Alps, a volcano-sedimentary sequence, metamorphosed under blueschist-facies conditions during the Alpine orogeny (Compagnoni et al. 1974; Manzotti et al. 2014), and considered to be Permo-Carboniferous in age. For the first time in the Western Alps, a detrital U–Pb zircon geochronological investigation combined with a lithostratigraphic study is applied to presumed Palaeozoic meta-sediments in order to decipher the maximum age of deposition and the provenance of the

detrital materials. The obtained results support the distinction of two different sedimentary formations within the Money Complex and allow discussing the palaeogeography of the Alpine region during the late Carboniferous and Permian times.

Geological setting

The Gran Paradiso Massif is attributed to the Briançonnais microcontinent (Schmid et al. 2004) and, together with the Monte Rosa and Dora-Maira, constitutes the Internal Massifs of the European Alps. They crop out as tectonic windows overthrust by eclogite-facies units, derived from the Liguria-Piemonte Ocean (Figs. 1, 2). The Gran Paradiso Massif comprises two units, the *Money Unit* and the overlying *Gran Paradiso Unit* (Compagnoni et al. 1974; Le Bayon et al. 2006).

The *Money Unit* is outcropping in the Money window below the overthrust Gran Paradiso Unit and is exposed in two valleys, namely the Valnontey and the Valeille (Fig. 2). The Money Unit consists of a late Palaeozoic leucogranite (Erfaulet meta-granite), actually located below a volcano-sedimentary sequence (Money Complex; Compagnoni et al. 1974). The Money Complex comprises (i) biotite-amphibole orthogneisses (Ballèvre 1988); (ii) paragneisses (meta-greywackes) with interlayered amphibolites (Le Bayon and Ballèvre 2006); and (iii) meta-sandstones with meta-conglomeratic layers (Amstutz 1962), and minor meta-pelites, some of them being rich in graphite (Compagnoni et al. 1974). It has been argued that the protolith age of the Money Complex is Permo-Carboniferous because of its lithology and the lack of high-temperature pre-Alpine relics in the detrital sequence (Compagnoni et al. 1974). At the boundary between the Erfaulet meta-granite and the Money Complex, the pre-Alpine garnet discovered in metapelites has been interpreted as the result of contact metamorphism (Le Bayon and Ballèvre 2004). In the Money Complex, a polyphased history has been recognized (Manzotti et al. 2014) with (i) evidence for the original volcano-sedimentary features and for magmatism occurring during the pre-Alpine evolution and (ii) four stages of Alpine deformation and metamorphism (from blueschist to albite-epidote amphibolite then greenschist-facies conditions). During the Alpine history, the Money Unit (Money Complex + Erfaulet meta-granite) has been deformed at regional scale by a hundred of metres in size, recumbent fold (Compagnoni et al. 1974; Le Bayon and Ballèvre 2006; Manzotti et al. 2014). This folding event also affected the tectonic contact between the Gran Paradiso and the Money Units (Manzotti et al. 2014).

The *Gran Paradiso Unit* is composed of augen-gneisses derived from porphyritic granitoids (Bertrand et al. 2005;

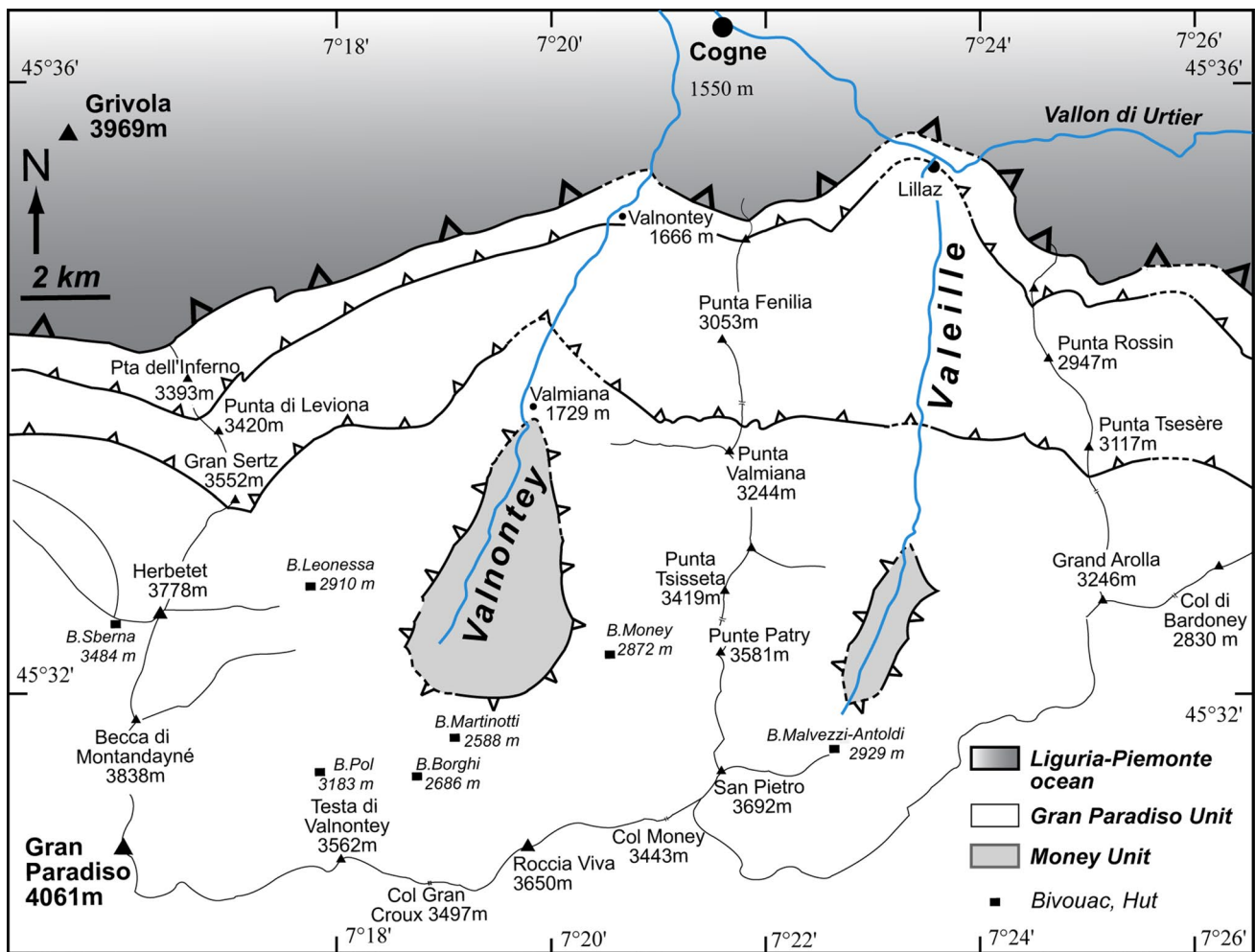


Fig. 2 Map of the northern part of the Gran Paradiso Massif: the Money Unit crops out in the Valnontey and Valeille valleys (modified after Le Bayon and Ballèvre 2006)

Ring et al. 2005) intruded into meta-sedimentary rocks (i.e. polymetamorphic paragneisses and micaschists). Lenses of mafic rocks, derived from late Palaeozoic gabbros (Pognante 1980; Gasco et al. 2010) and from pre-Alpine amphibolites (Compagnoni and Lombardo 1974; Battiston et al. 1984; Benciolini et al. 1984; Dal Piaz and Lombardo 1986; Ballèvre 1988; Brouwer et al. 2002), are found in the paragneisses. The pre-Triassic basement is overlain by thin remnants of a Mesozoic meta-sedimentary cover (Elter 1960, 1972; Polino and Dal Piaz 1978).

Regional amphibolite-facies metamorphism (4–6 kbar, 600–650 °C, Le Bayon and Ballèvre 2006) is recorded in metasediments, whereas contact metamorphism (2.6 ± 0.5 kbar, 640–680 °C) is recognizable along intrusive contacts (Compagnoni and Prato 1969; Compagnoni et al. 1974; Gabudianu Radulescu et al. 2011). A variety of lithologies preserves evidence for an eclogite-facies metamorphism (Compagnoni and Lombardo 1974; Dal

Piaz and Lombardo 1986; Le Goff and Ballèvre 1990; Le Bayon et al. 2006). The minimum P–T conditions were estimated at 12–14 kbar at 500–550 °C, whereas in the Al- and Mg-rich micaschists (e.g. “whiteschists” or “silvery micaschists”), P–T conditions of 21–23 kbar at 540–570 °C have been proposed for this stage (Vidal et al. 2001; Wei et al. 2003; Le Bayon et al. 2006; Gabudianu Radulescu et al. 2011). The eclogite-facies metamorphism was followed by a late retrogression under epidote amphibolite to greenschist-facies stage (Le Bayon et al. 2006).

The Money Complex

The Money Unit consists of the Erfauel meta-granite and the Money Complex, a volcano-sedimentary sequence. The main characteristics of the Money Complex and its depositional settings will be presented in the following section.

Lithological, petrographical, and stratigraphical data

In the Money Complex, a graphite-bearing meta-sedimentary formation, which includes thick layers of meta-conglomerates, was identified by Amstutz (1962) and Compagnoni et al. (1974). Detailed mapping of the Money Unit allowed distinguishing two detrital meta-sedimentary formations: a *polygenic graphite-rich meta-sedimentary formation* and a *monogenic graphite-poor meta-sedimentary formation* (Manzotti et al. 2014). These two detrital meta-sedimentary formations are physically separated from each other by (i) fine-grained, *biotite-amphibole-bearing orthogneisses*, up to 50 m thick, probably deriving from alkaline volcanics and (ii) *albite-bearing paragneisses* (20–50 m thick), with *amphibolite* layers. Both the *polygenic* and the *monogenic meta-sedimentary formations* display matrix-supported meta-conglomeratic layers, but differ in (i) the internal stratigraphic organization, (ii) the distribution of graphite, (iii) the structural position, and (iv) the nature and amount of pebbles that form the meta-conglomeratic layers (Manzotti et al. 2014).

The *polygenic meta-sedimentary formation* best outcrops between the right-side moraine of the Money Glacier and the rocky cliffs lying immediately below the actual front of the glacier. Because of the ice retreat since the end of the Little Ice Age, the polished surfaces have been uncovered, allowing for excellent exposure. It comprises cm- to m-thick grey to black layers of graphite-micaschists (i.e. former organic-rich mudstones) alternating with light grey layers (0.1–1 m thick) of quartz-rich micaschists (i.e. former organic-rich arenites) and grey layers of matrix-supported meta-conglomerates (0.2–0.6 m thick) (Fig. 2a, b). The matrix-supported meta-conglomerates mostly contain abundant elongated lenses (up to 5 cm in size) of (i) monomineralic quartz aggregates, (ii) fine-grained, leucocratic gneisses, (iii) fine-grained micaschist, (iv) coarse-grained gneisses, and (v) dark, graphite-rich lenses (Fig. 2c, d). These lenses could derive from former pebbles of quartz veins, aplites, siltstones or sandstones, granites, and carbon-rich mudstones, respectively.

When identifiable, the sedimentary layering shows that the meta-conglomeratic levels are interlayered within finer-grained rocks, the amount of conglomerates being approximately equal to the amount of sandstones/siltstones. In this formation, graphite is present everywhere.

The *monogenic meta-sedimentary formation* outcrops on both sides of the Valnontey valley and is especially well exposed around the former Money village. It mainly consists of matrix-supported angular to rounded quartz-pebble meta-conglomerates (up to 5 m thick) intercalated with quartz-micaschist layers (0.1–0.3 m thick) (Fig. 3a, b). They frequently display a grey or brown weathering colour, with reddish brown bands and domains (Fig. 4c).

The quartz-rich matrix of the meta-conglomerates mostly contains white mica, garnet, and locally biotite, chlorite, and chloritoid. Other types of pebbles (e.g. aplites) are rare (Fig. 4d). Quartz pebbles, representing former nodules of quartz veins, range from 1 cm to 20 cm in diameter and are frequently elongated along with the Alpine structures (i.e. foliation and lineation) (Fig. 4b). Detrital garnet grains, corroded as a consequence of abrasion and dissolution, have been described in these matrix-supported meta-conglomerates (Manzotti and Ballèvre 2013).

Locally, the original bedding is still well defined by thin layers (0.1–0.3 m thick) of fine-grained meta-sediments (former sandstones or siltstones) and by the intercalation of quartz-micaschist and of quartz-pebble meta-conglomerates (Fig. 4a). The quartz-micaschist layers mainly consist of white mica, quartz, garnet, albite, graphite (~5 %), chlorite, and locally biotite, chloritoid. The main Alpine foliation is marked by quartz-rich layers and by the shape-preferential orientation of white mica, locally chloritoid and more rarely graphite.

Depositional setting

Taking into account the whole set of field data, the sedimentary sequence now making the Money Complex consists, from base to top, of (i) the polygenic sedimentary formation, (ii) the alkaline volcanics, (ii) greywackes with interbedded mafic volcanics, and finally (iv) the monogenic sedimentary formation (Fig. 5).

Although the outcrop conditions are fairly good, the polyphased Alpine deformation makes it difficult to describe the depositional features for the conglomeratic layers in both the mono- and polygenic meta-sedimentary formations. Nevertheless, some layers show lenticular shapes: They may represent channels filled by coarse-grained material, which developed in a continental fluvial environment. The biotite-amphibole-bearing orthogneiss, the albite-bearing paragneiss (meta-greywackes), and the amphibolites may be interpreted as volcanic or volcano-sedimentary episodes that occurred between the deposition of the two sedimentary formations.

Again, because of the Alpine deformation, it is difficult to assess the polarity of the two meta-sedimentary formations as both the graded bedding and the erosive bases are poorly preserved. Furthermore, the outcrop discontinuities bring some limitation in the interpretation, and way-up criteria need to be determined not only at the scale of the single outcrop, but at the scale of the meta-sedimentary formation. In the polygenic meta-sedimentary formation, polished surfaces at the foot of the Money Glacier display well-stratified sequences, where individual meta-conglomeratic layers sometimes display clear-cut evidence of graded bedding (Fig. 3a). In these outcrops, the polarity is normal. In the monogenic meta-sedimentary formation,

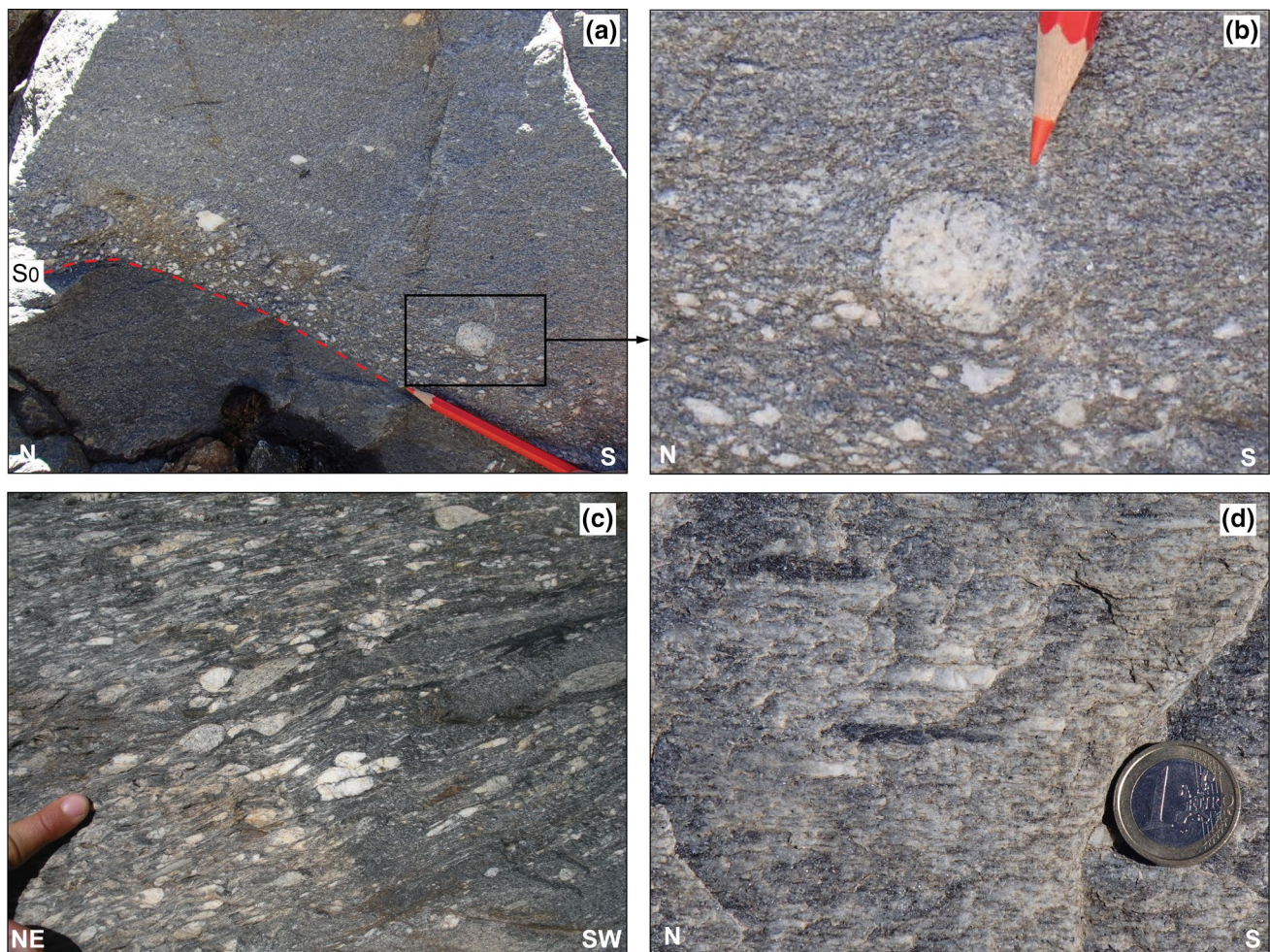


Fig. 3 Field aspect of the polygenic meta-sedimentary formation. UTM ED 1950 coordinates for each photograph are given. **a** Stratigraphic contact between meta-conglomeratic layers and a cm-thick band of graphite-micaschists (370364/5044483). **b** Detail of the previous picture, showing a sub-rounded granitic pebble (2 cm in size) and several sub-angular quartz pebbles in a matrix-supported meta-

conglomeratic layer. **c** Elongated pebbles of quartz, fine-grained leucocratic, aplitic gneisses, coarse-grained granitic gneisses, and fine-grained micaschist (up to 5 cm in size) (370,325/5,044,483). **d** Graphite-rich lenses that may represent former mud clasts (370,306/5,044,469)

way-up criteria have not been found, except in one locality along the footpath to the Herbetet hut. There, the sequence is inverted because conglomerates are far more abundant within the monogenic meta-sedimentary formation close to the albite-bearing paragneisses, and because the coarsest layers are in contact with the albite-bearing paragneisses. These observations suggest that the deposits are fining upwards and that the monogenic meta-sedimentary formation was deposited above the albite-bearing paragneisses.

As a whole, field observations are consistent with a model where the first sequence is made of polygenic conglomerates, suggesting a close source for the detrital material. After a volcanic episode, the second sequence would have been deposited in a more mature environment, further away from the source or in a more aggressive climate (because only quartz pebbles, the most resistant material, are present).

Analytical methods

The samples were crushed using a SELFRAG apparatus to a maximum grain size of ~250 µm. Zircon grains were separated at the University of Bern (Switzerland) using a Frantz magnetic separator, panning and heavy liquid techniques (density 3.32 g/cc). Finally, zircon grains were hand-picked under a binocular microscope. The grains for LA-ICP-MS analysis were mounted in one-inch epoxy resin pucks and polished down to expose the centre of the grains. Zircon grains different in shape, size, and colour were selected in order to avoid hand-picking bias (Sláma and Košler 2012). The growth textures of the sectioned grains were studied by cathodoluminescence (CL) imaging, using a Reliontron CL system equipped with a digital colour camera available in Géosciences Rennes and following the

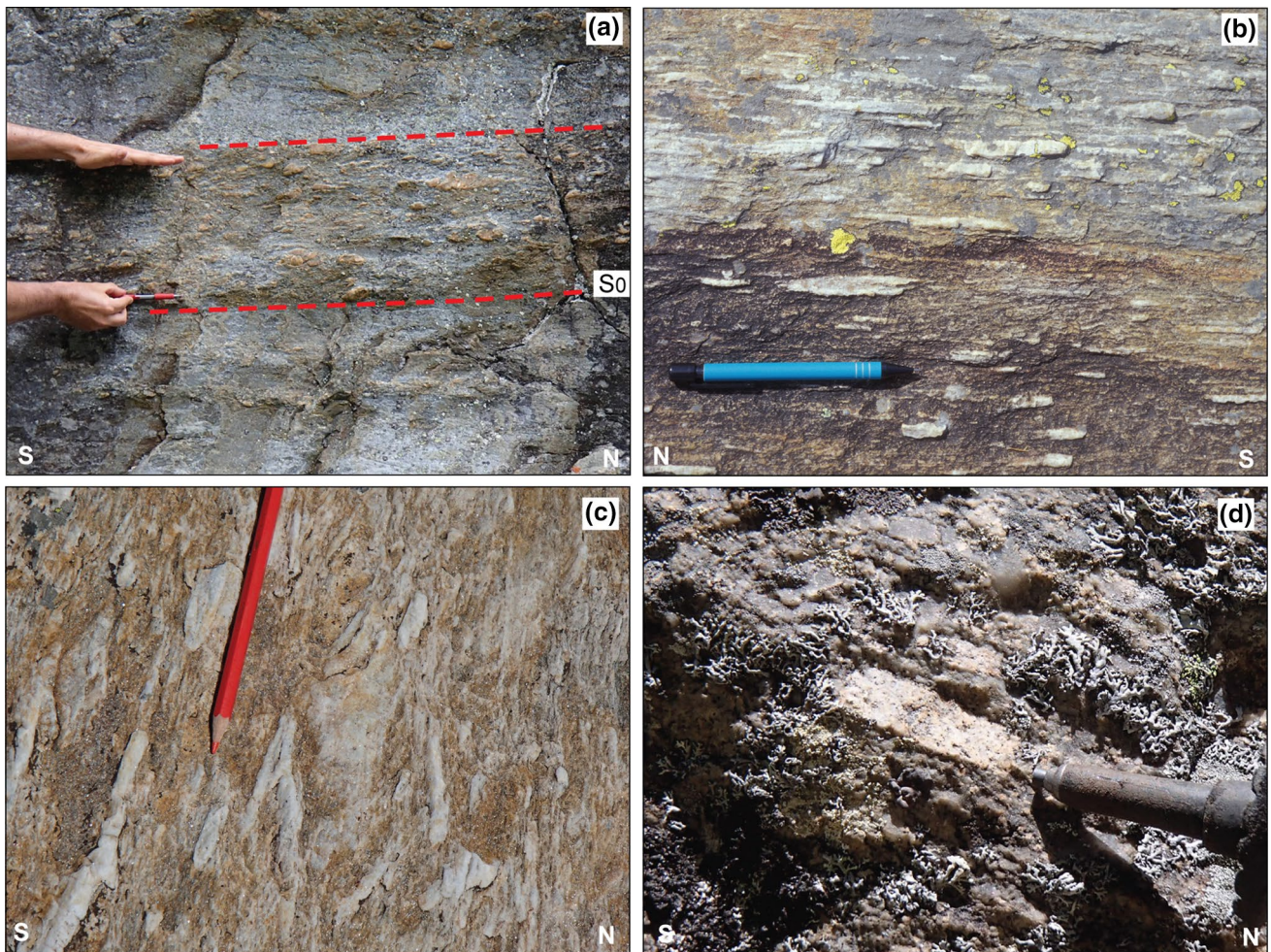


Fig. 4 Field aspect of the monogenic meta-sedimentary formation. UTM ED 1950 coordinates for each photograph are given. **a** 20-cm-thick layers alternate to quartz-micaschist bands in stratigraphic contact (368,641/5,044,940). **b** Quartz lenses (up to 5 cm long) in a

quartz-rich matrix (368,504/5,045,186). **c** Quartz meta-conglomerates deformed during the Alpine history. Quartz pebbles folded and strongly stretched parallel to the lineation (369,480/5,045,347). **d** Angular aplitic pebbles (3 cm in size) (369,016/5,045,837)

approach suggested by Rubatto and Gebauer (2000) and Corfu et al. (2003). The study of the zircon morphology and specifically the grade of roundness has been performed following the classification proposed by Powers (1953), adapted for heavy minerals.

Both cores and rims of zircon grains were analysed by LA-ICP-MS at the Geosciences Rennes laboratory (University of Rennes 1). Ablation was performed using a ESI NWR193UC, powered by an ultra-short pulse Coherent Excistar XS Excimer laser system operating at a wavelength of 193 nm, and consisted of 16-, 25-, and 30- to 40- μm spot diameters (depending on the size of the mineral zone targeted) produced with a repetition rate of 3 Hz. Ablated material was carried to the mass spectrometer in He (~0.8 l/min) and then mixed with N (0.04 l/min) and Ar (~0.85 l/min), before being introduced to the ICP source of an Agilent 7,700 \times quadrupole ICP-MS equipped with a

dual pumping system to enhance sensitivity. Tuning of the instrument and mass calibration were performed before the analytical session using the NIST SRM 612 reference glass, by monitoring the ^{238}U signal and minimizing the ThO^+/Th^+ ratio (<0.5 %). Analyses consisted in the acquisition of the $^{204}(\text{Pb} + \text{Hg})$, ^{206}Pb , ^{207}Pb , ^{208}Pb , ^{232}Th , and ^{238}U signals. The ^{235}U abundance was calculated from the measured ^{238}U on the basis of a $^{238}\text{U}/^{235}\text{U}$ ratio of 137.88. Single-spot analyses consisted of ~20 s of background integration with the laser off, followed by ~60 s integration with the laser firing, and then a ~10 s delay for wash out. Raw data were corrected for Pb/U and Pb/Th laser-induced elemental fractionation and for instrumental mass discrimination by standard bracketing with repeated measurements of the zircon reference material GJ-1 (Jackson et al. 2004). Along with the unknowns, the 91,500 standard zircon (Wiedenbeck et al. 1995, 2004) was measured to monitor

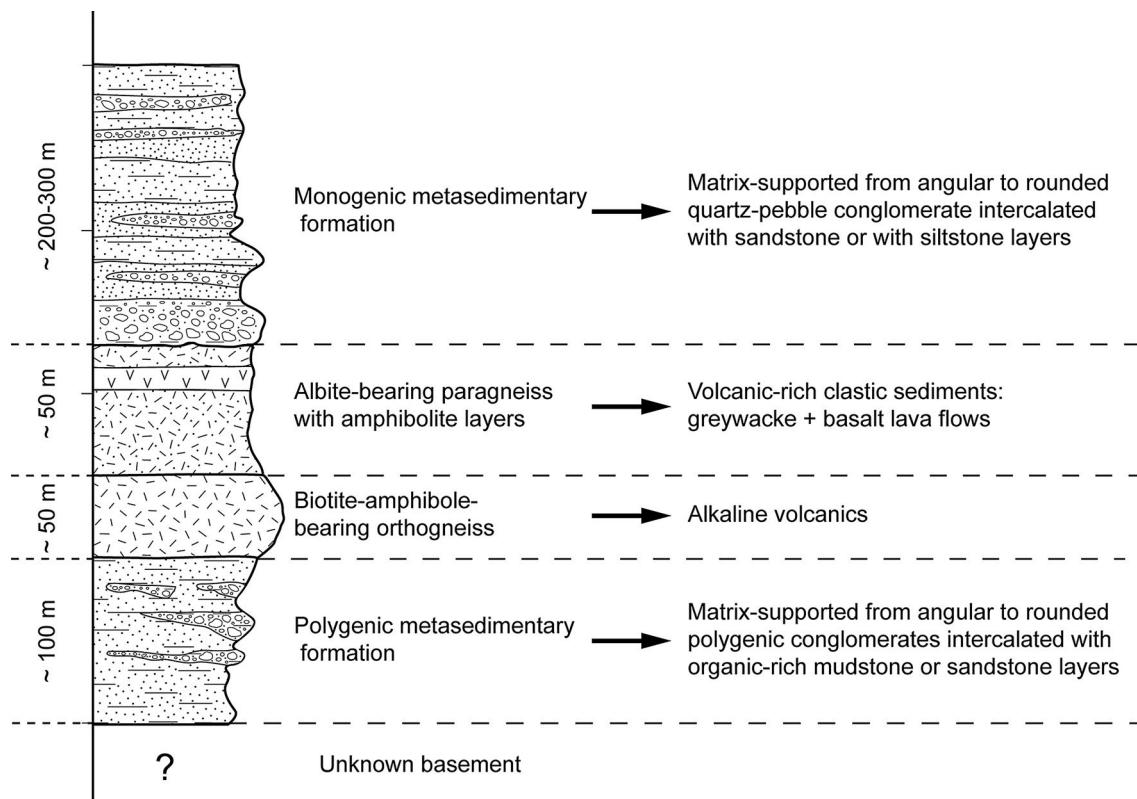


Fig. 5 Lithostratigraphic column of the Money Complex

precision and accuracy of the analyses and produced a concordia age of $1,063.7 \pm 4.9$ Ma ($N = 13$, MSWD = 0.75) during the course of the analyses. Data reduction was carried out with the GLITTER software package (Van Achterbergh et al. 2001; Jackson et al. 2004). The analyses were performed in time resolved mode.

Isotopic ratios and single ages are reported with 1σ errors, whereas mean ages are given at the 95 % confidence level (c.l.). Both core and rim domains were analysed. The complete isotopic dataset is listed in Supplementary data Tables 2 and 3. Single-spot analyses are given as $^{207}\text{Pb}/^{206}\text{Pb}$ ages for results ≥ 1 Ga and $^{206}\text{Pb}/^{238}\text{U}$ ages for results < 1 Ga (see Faure and Mensing (2005) and Talavera et al. (2012) for an explanation of the used method).

Ages were calculated using Isoplot (Ludwig 2003) and plotted as kernel density diagrams generated by the DensityPlotter program (Vermeesch 2012). This program is based on a standard statistical technique called kernel density estimation (KDE), which involves summing a set of Gaussian distributions, but does not explicitly take into account the analytical uncertainties (Vermeesch 2012). The advantage with respect to the Probability Density Plot (i.e. the most widespread method for visualizing detrital age distributions) is to avoid the possibility to produce counter-intuitive results when data quantity (number of

analyses) and/or quality (precision) are high (Vermeesch 2012). To reduce the risk of bias in detrital zircon geochronology, the protocol described by Malusà et al. (2013) has been followed: (i) in order to minimize the risk of missing provenance components, both concordant and discordant ages were reported in kernel density diagrams (Fedó et al. 2003; Nemchin and Canwood 2005; Vermeesch 2012); (ii) the Kolmogorov–Smirnov test (Smirnov 1939; Young 1977; Vermeesch 2013) has been used (significance level $\alpha = 0.05$) in order to quantify the effects induced by variable cut-off level of discordant grain ages and to assess the similarity between the distribution of the analysed samples (if $V_{k-s} > 0$, differences between distributions are statistically not significant; see Malusà et al. 2013); and (iii) relationships between grain shape and U concentration, between grain shape and age, have also been examined.

Morphological, textural, chemical study and U–Pb dating of zircon grains

Two samples were analysed for detrital zircon studies: one sample belongs to the polygenic graphite-rich metasedimentary formation (MN1228A—UTM ED 1950 coordinates: 369,836–5,044,172) and the other one to

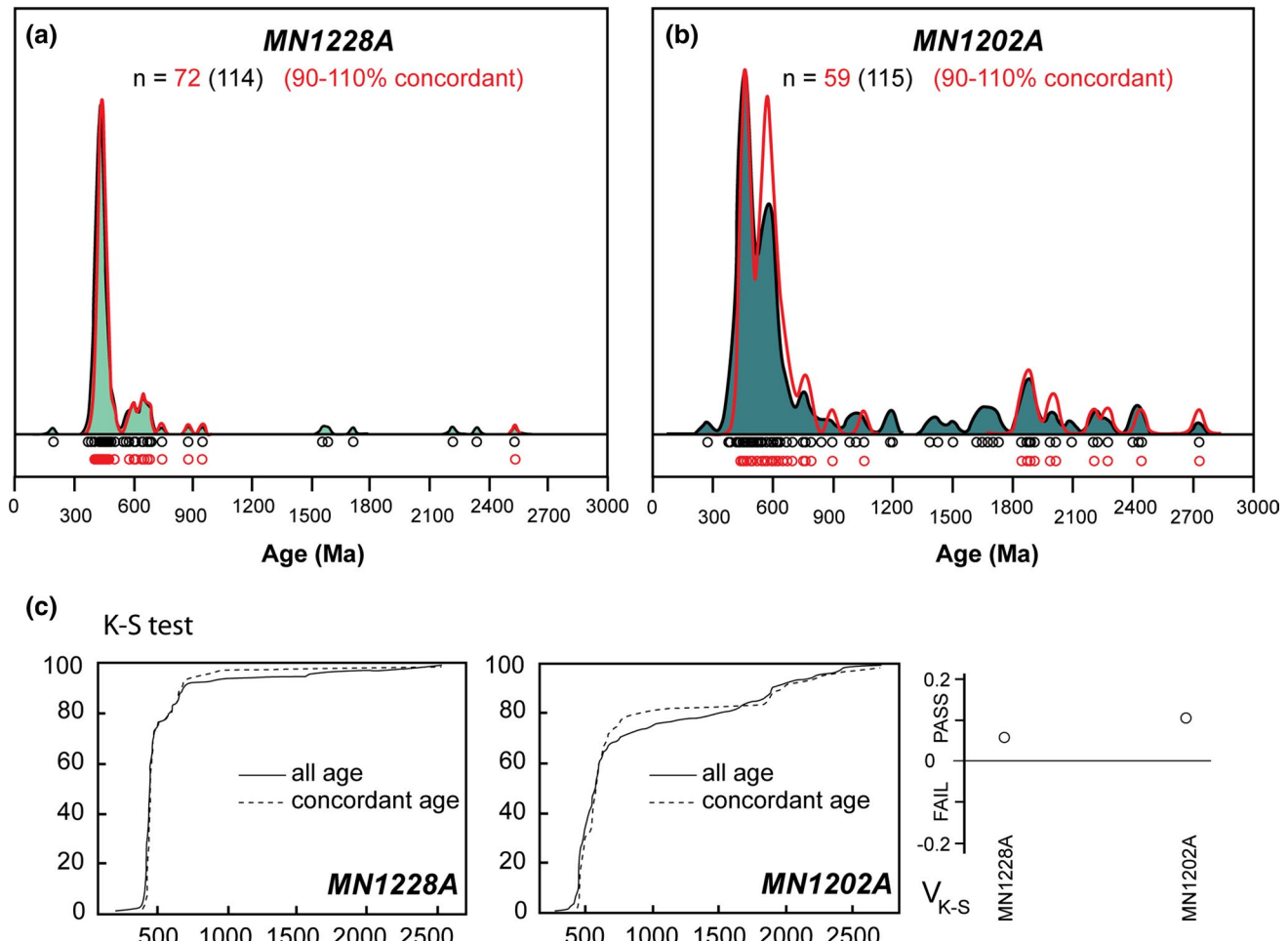


Fig. 6 **a, b** Coloured areas represent kernel density estimates for all grain ages (indicated by black circles in the upper row). Red lines are kernel density estimates calculated for grain ages <10 % discordance (red circles in the lower row are single grain ages). Single-spot analyses are given as $^{207}\text{Pb}/^{206}\text{Pb}$ ages for results older than 1 Ga and $^{206}\text{Pb}/^{238}\text{U}$ ages for results younger than 1 Ga. **a** Sample MN1228 from the polygenic meta-sedimentary formation. **b** Sample MN1202A from the monogenic meta-sedimentary formation. **c** Simi-

larities between distributions of all grain ages, and grain ages <10 % discordant is evaluated by the K-S method (comparison between the maximal distance between cumulative frequency curves (bottom) with the critical value for a 0.05 significance level. Note that the differences between the all zircon ages and the concordant ages are not statistically significant ($V_{K-S} > 0$) in both samples (cf. Malusà et al. 2013)

the monogenic graphite-poor meta-sedimentary formation (MN1202A—UTM ED 1950 coordinates: 368,642–5,044,943). No zircon grains were found in the alkaline orthogneiss and the Erfauft meta-granite as already noticed by Bertrand et al. (2005).

Polygenic meta-sedimentary formation

MN1228A is a graphite-micaschist with interbedded layers of meta-conglomerates. The graphite-micaschist consists of white mica (~25 %), graphite (~20 %), albite (~10 %), quartz (~10 %), garnet (~10 %), chlorite (~10 %), titanite (~5 %), biotite (~5 %), and blue-green amphibole (<5 %). Zircon, rutile, and ilmenite are found as accessory phases.

A total of 114 Zircon grains were analysed in this sample, 72 of which yielded concordant dates ranging from $2,539 \pm 11$ Ma down to 407.5 ± 4.7 Ma (Fig. 6a). The differences between the distributions of concordant and discordant dates are not statistically significant ($V_{K-S} > 0$, Fig. 6c). All zircon grains are inclusion-free, ~24 % are slightly rounded, and ~11 % are rounded (Fig. 7a). Most of the zircon grains are pink, and few are colourless. The CL imaging allow recognizing (i) grains with oscillatory magmatic zoning, (ii) grains with partially dissolved cores surrounded by younger (magmatic or metamorphic) overgrowths, and (iii) homogenous grains.

Zircon grain sizes (expressed as the equivalent spherical diameter, i.e. the cube root of the product of the three

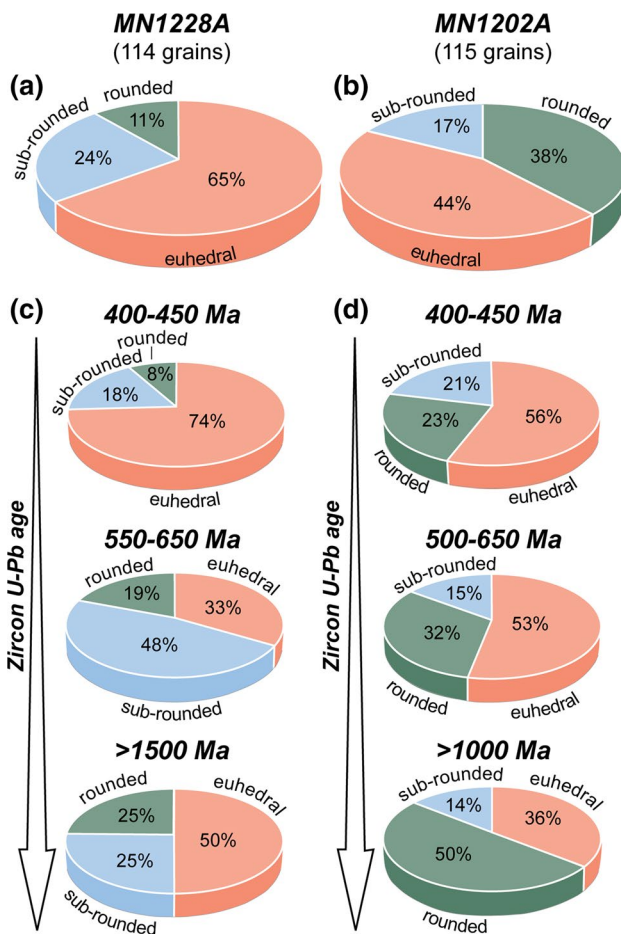


Fig. 7 Pie charts (a, b) comparing the amount of rounded versus sub-rounded versus euhedral zircon grains and illustrating relationships between grain shape and $^{206}\text{Pb}/^{238}\text{U}$ ($<1\text{ Ga}$) or $^{207}\text{Pb}/^{206}\text{Pb}$ ($>1\text{ Ga}$) age of zircon crystals in sample MN1228A (polygenic meta-sedimentary formation) and MN1202A (monogenic meta-sedimentary formation), respectively. c and d Pie charts comparing the amount of rounded versus sub-rounded versus euhedral zircon grains within the main U-Pb age populations of Fig. 8

axis lengths) range between 2.73Φ ($150 \mu\text{m}$) and 4.04Φ ($61 \mu\text{m}$) (Fig. 8a).

The relations between the grain size and the grain age of the detrital zircon U-Pb dataset for sample MN1228A are shown in Fig. 8a. Roughly, two main U-Pb age clusters parallel to the y-axis and with the main concentration at ca 450–400 Ma and 650–550 Ma, respectively, are recognizable. Considering all the data (i.e. concordant and discordant), these two U-Pb age groups do not show (i) significant differences between grain-age distributions in different grain-size classes and (ii) relations between grain age and grain size. This ensures that the age distributions are not influenced by hydraulic sorting effects or any other bias introduced during sample processing (Malusà et al. 2013). A third group, distributed on a larger age span (between 2,550 and 1,500 Ma, $^{207}\text{Pb}/^{206}\text{Pb}$ ages) with respect to the

two younger clusters, can be identified: It comprises detrital zircon crystals, characterized by relatively uniform grain size (corresponding to very fine sand, Fig. 8a). The three main age groups recognized in sample MN1228A display different ratios of euhedral versus sub-rounded versus rounded grains (Fig. 3a). The percentage of rounded grains slightly increases in the older groups (8 % in the 400–450 Ma age cluster, 19 % in the 550–650 Ma age cluster, and 25 % in the 1,500–2,550 Ma age cluster). Rounded, sub-rounded, and euhedral zircon crystals show the same statistical U concentration distribution (Fig. 9a). U-rich zircon grains occur only in the younger U-Pb age group (450–400 Ma) (Fig. 9b), implying that the oldest U-rich grains were probably metamict and selectively destroyed (Malusà et al. 2013).

The analysed zircon grains mainly derived from metamorphic (45 grains) and subordinately from mafic magmatic sources (28 grains), with only a minor contribution from felsic magmatic sources, as suggested by their calculated Th/U ratios (see Heaman et al. (1990), Schaltegger et al. (1999), Vavra et al. (1999), Rubatto (2002), Teipel et al. (2004) and Linnemann et al. (2011) for an explanation of the used method) (Fig. 10a, b). Metamorphic dates present the same statistical distribution in the homogenous grains (56 %), rims, and overgrowths (44 %) (Fig. 11). Metamorphic grains are mostly euhedral (67 %), while ~24 % are sub-rounded and only ca 9 % are rounded (Fig. 11). Twenty-six of the forty-five metamorphic grains yielded concordant Ediacaran and Silurian dates, ranging from $600 \pm 7\text{ Ma}$ down to $417 \pm 5\text{ Ma}$. In detail, 24 of these dates clustered into one Silurian population with a mean concordia age of $440 \pm 7\text{ Ma}$, whereas two of these dates are older (Ediacaran) at 600 ± 7 and $577 \pm 6\text{ Ma}$, respectively. The Silurian grains are euhedral (63 %), sub-rounded (25 %), and rarely rounded (12 %), with sizes ranging from 3.62Φ ($81 \mu\text{m}$) to 2.85Φ ($139 \mu\text{m}$). Metamorphic discordant dates are equally associated to homogenous grains and to rims and overgrowths.

Mafic magmatic zircon grains present magmatic oscillatory zoning with only a few with younger magmatic overgrowths around older, locally partially dissolved, cores (Fig. 12). Considering all the mafic magmatic crystals, they are mostly euhedral (55 %), sub-rounded (24 %), and rounded (21 %). Sixteen out of the 29 magmatic zircon grains derived from mafic magmatic sources yielded concordant dates ranging from Neoarchean ($2,539 \pm 11\text{ Ma}$; $N = 1$, $^{207}\text{Pb}/^{206}\text{Pb}$ age) to Silurian ($438 \pm 5\text{ Ma}$, $^{206}\text{Pb}/^{238}\text{U}$) (Fig. 12). They include (i) Palaeoproterozoic (6 %), (ii) Neoproterozoic (63 %), and (iii) Palaeozoic (31 %) dates. The Neoproterozoic dates include (i) two Tonian grains ($949 \pm 11\text{ Ma}$, $878 \pm 10\text{ Ma}$), (ii) six Cryogenian grains ($743 \pm 8\text{ Ma}$ to $638 \pm 7\text{ Ma}$), and (iii) two Ediacaran grains ($610 \pm 7\text{ Ma}$, $602 \pm 7\text{ Ma}$). The Cryogenian grains are

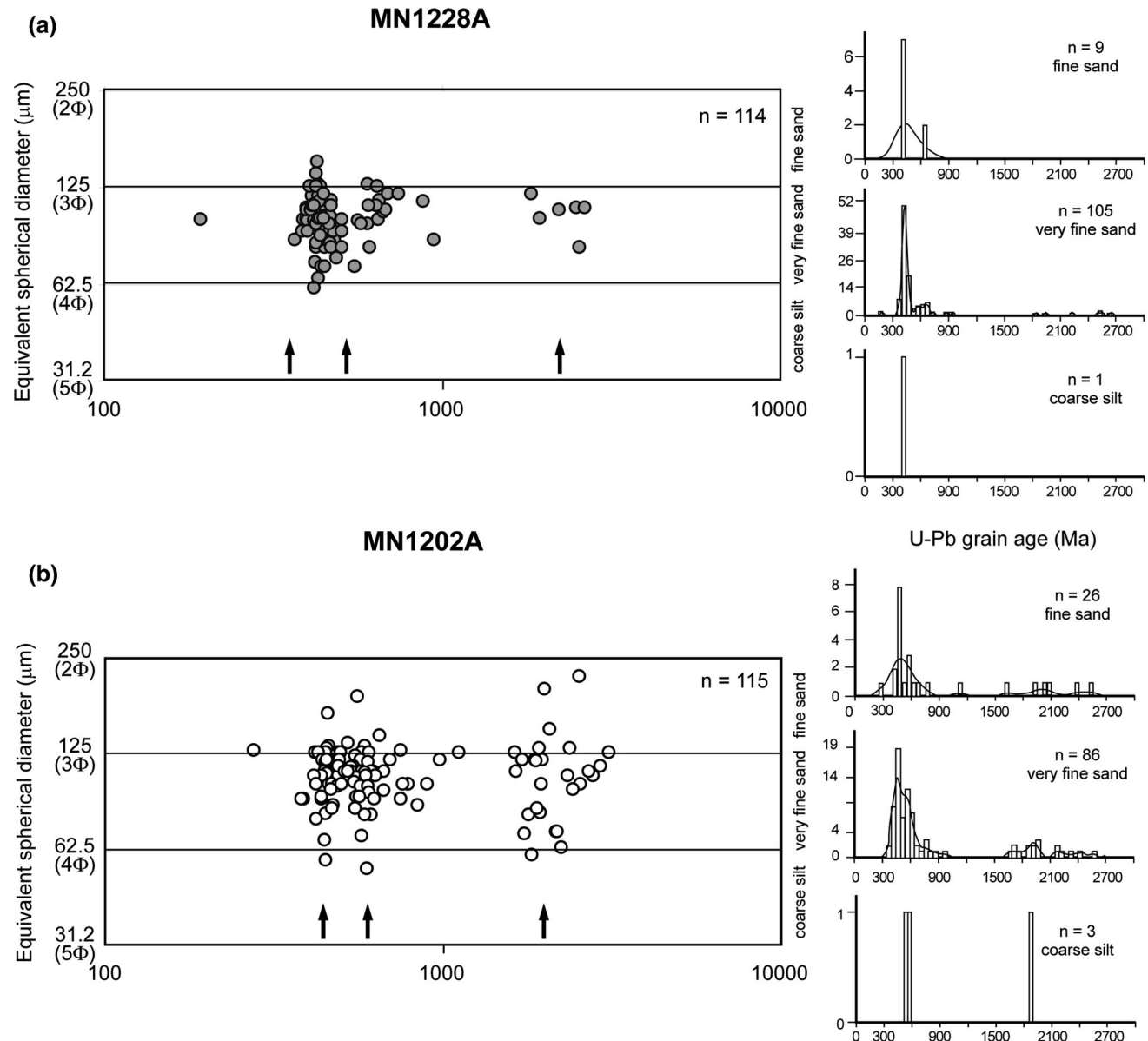


Fig. 8 Equivalent spherical diameter versus grain age in detrital zircon grains from the two meta-sedimentary formations of the Money Complex. **a** Sample MN1228A from the polygenic meta-sedimentary formation. **b** Sample MN1202A from the monogenic meta-sedimentary formation. The equivalent spherical diameter is the cube root of the product of the three zircon axis lengths (measured at the microscope and assuming that the third axis is equal to the grain width).

In this diagram, the *black arrows* indicate the recognized three age clusters (note that in both samples, the oldest $^{207}\text{Pb}/^{206}\text{Pb}$ age group is less well defined and distributed on a larger age span). On the right, kernel density estimates and histograms showing the age distribution in different grain-size classes (fine sand, very fine sand, and coarse silt) within the 0–2,700 Ma range

euhedral (70 %) and rarely sub-rounded (20 %) or rounded (10 %). Their sizes vary from 3.33Φ (99 μm) to 2.98Φ (126 μm). Two grains were Cambrian with a mean concordia age of 505 ± 8 Ma, one is Ordovician (469 ± 7 Ma), and the two younger grains are Silurian in age with a mean date of 439 ± 7 Ma (Fig. 12). The Cambrian grains show similar sizes (92–99 μm equivalent to $3.43\text{--}3.33 \Phi$).

Monogenic meta-sedimentary formation

MN1202A is a micaschist with minor quartz meta-conglomeratic intercalations. This micaschist mostly consists of white mica (~45 %), quartz (~25 %), garnet (~15 %), chloritoid (5 %), chlorite (5 %), and graphite (<5 %). Zircon, rutile, and ilmenite are the main accessory minerals.

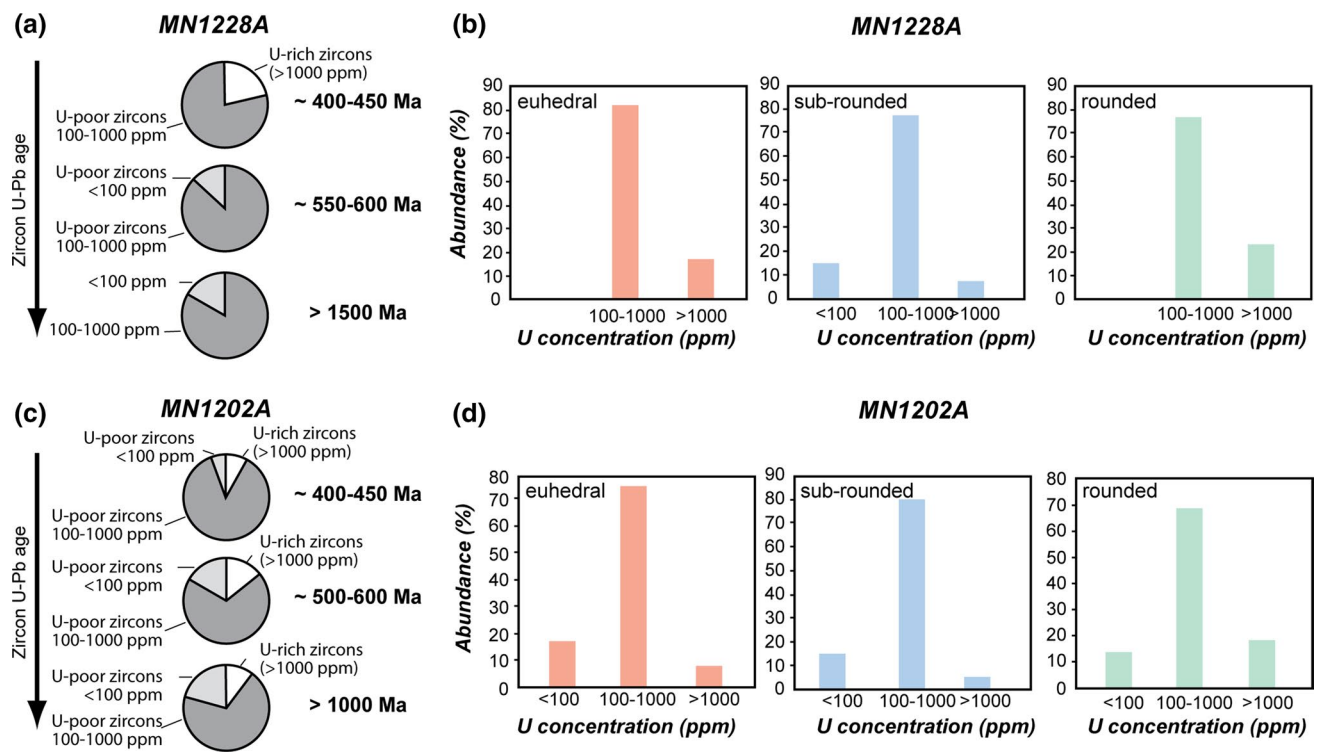


Fig. 9 **a–c** Relationships between U concentration and $^{206}\text{Pb}/^{238}\text{U}$ ($<1 \text{ Ga}$) or $^{207}\text{Pb}/^{206}\text{Pb}$ ($>1 \text{ Ga}$) age in zircon grains from the two meta-sedimentary formations of the Money Complex. Pie charts comparing the amount of U-rich ($>1,000 \text{ ppm}$) versus U-poor ($100\text{--}1,000 \text{ ppm}$ and $<100 \text{ ppm}$, respectively) zircon grains within the main U–Pb age populations of Fig. 8. Note that in sample MN1202A,

U-rich zircon grains systematically decrease in the older U–Pb age groups. **b–d** Histograms of U concentrations in euhedral, sub-rounded, and rounded zircon grains, showing a similar statistical distribution in grains with different shape. **a** and **b** Sample MN1228A from the polygenic meta-sedimentary formation. **c** and **d** Sample MN1202A from the monogenic meta-sedimentary formation

A total of 114 grains were selected from this sample, 59 of which yielded concordant dates ranging from $2,720 \pm 12 \text{ Ma}$ down to $439 \pm 5 \text{ Ma}$ (Fig. 6b). The differences between the distribution of concordant and discordant dates are not statistically significant ($V_{K-S} > 0$, Fig. 6c).

Zircon grains are inclusion-free, 38 % are slightly rounded, and ca 17 % are rounded (Fig. 7b). Most of the zircon grains are colourless and occasionally pink. The CL imaging shows (i) partially dissolved cores with younger (magmatic or metamorphic) overgrowths, (ii) homogenous grains, or (iii) grains with typical magmatic oscillatory zoning.

The grain sizes vary between 2.18Φ ($220 \mu\text{m}$) to 4.20Φ ($54.3 \mu\text{m}$) (Fig. 8b). The few pink grains are rounded with sizes ranging from 2.18Φ ($220 \mu\text{m}$) to 2.32Φ ($200 \mu\text{m}$).

The relations between the grain size and the grain age of the detrital zircon U–Pb dataset for sample MN1202A are presented in Fig. 8b. Two main U–Pb age clusters parallel to the y-axis are recognizable: They display the main concentration at about 450–400, 650–500 Ma. An older less well-defined group, characterized by a large age range (from 2,720 down to 1,000 Ma, $^{207}\text{Pb}/^{206}\text{Pb}$ ages), can be identified. Considering all the concordant and discordant

data, there are no (i) significant differences between grain-age distributions in different grain-size classes and (ii) relations between grain size and grain size, suggesting that the age distributions is not influenced by hydraulic sorting effects or any other bias introduced during sample processing.

The main age groups recognized in sample MN1202A display different ratios of euhedral versus sub-rounded versus rounded grains (Fig. 7b), with the percentage of rounded grains increasing in the older age groups. Rounded, sub-rounded, and euhedral grains display the same statistical distribution of U concentrations (Fig. 8a). U-rich zircons are mostly characterized by the same statistical distribution within the main age groups (Fig. 9b).

The Th/U ratios (see Heaman et al. (1990), Schaltegger et al. (1999), Vavra et al. (1999), Rubatto (2002), Teipel et al. (2004) and Linnemann et al. (2011) for an explanation of the used method) measured in the analysed zircon grains indicate that they dominantly derive from mafic magmatic sources (52 grains), with minor contributions from felsic magmatic and metamorphic (19 metamorphic grains) sources (Fig. 10c, d). Mafic magmatic data are associated with (i) a majority of grains characterized by

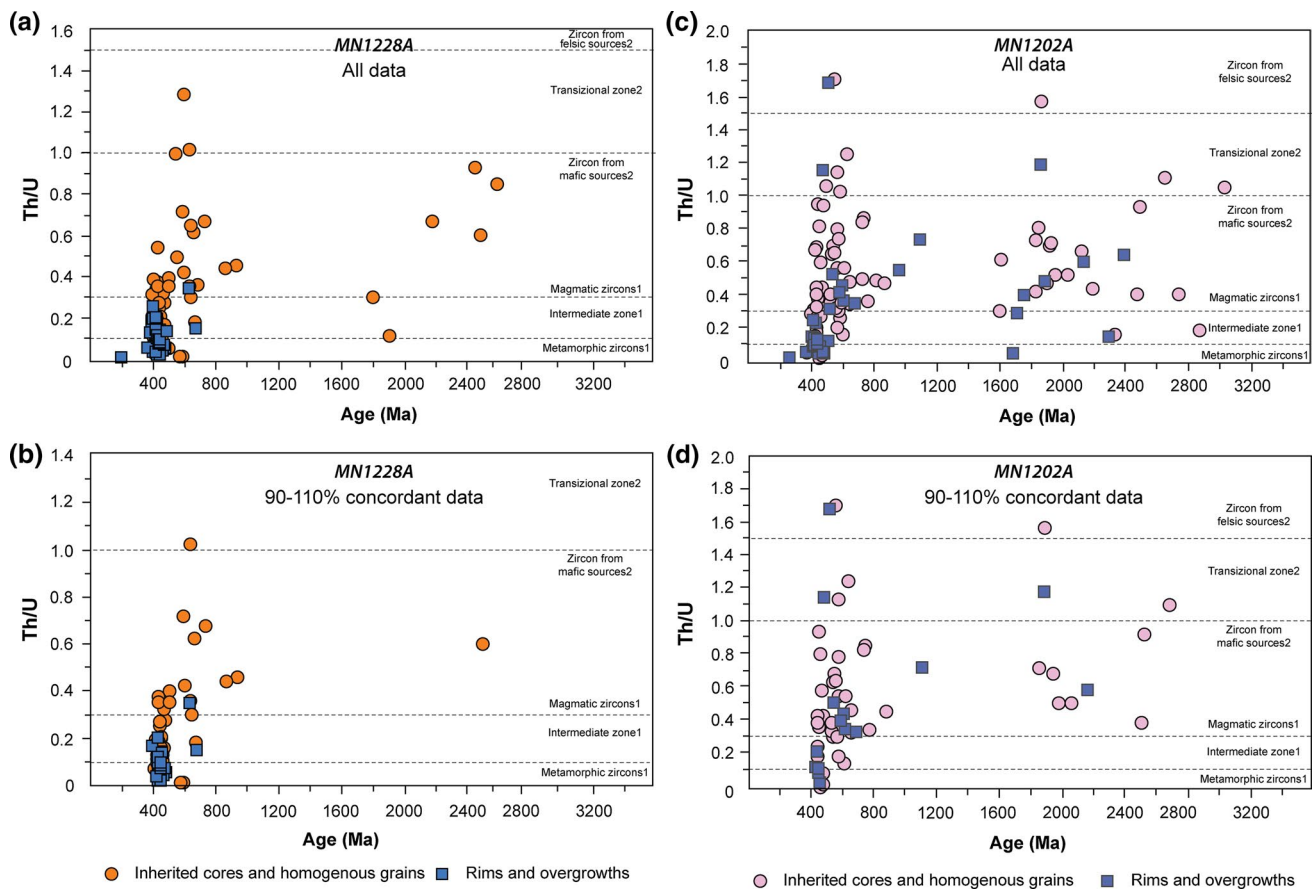


Fig. 10 **a** Zircon Th/U ratio versus age plot for sample MN1228A (polygenic meta-sedimentary formation) of the Money Complex. The majority of the grains derive from metamorphic sources. **b** Zircon Th/U ratio versus age plot for sample MN1228A (polygenic meta-sedimentary formation) of the Money Complex: only grain ages <10 % discordance are plotted. **c** Zircon Th/U ratio versus age plot for sample MN1202A (monogenic meta-sedimentary forma-

tion) of the Money Complex. The majority of grains derive from metamorphic sources. **d** Zircon Th/U ratio versus age plot for sample MN1202A (monogenic meta-sedimentary formation) of the Money Complex: only grain ages <10 % discordance are plotted. Superscript 1 refers to magmatic versus metamorphic zircon fields as proposed by Teipel et al. (2004), whereas superscript 2 refers to mafic versus felsic zircon sources fields as proposed by Linnemann et al. (2011)

magmatic oscillatory zoning, (ii) younger magmatic overgrowths surrounding older partially dissolved cores, and (iii) few homogenous grains. Considering all the mafic magmatic grains, they are either euhedral (52 %), rounded (36 %), or sub-rounded (13 %) (Fig. 13). Thirty-four out of the 52 mafic magmatic grains yielded concordant dates which are Neoarchean to Ordovician in age, ranging from $2,554 \pm 17$ Ma down to 454 ± 5 Ma (Fig. 13). The Meso-proterozoic dates include Neoarchean ($2,554 \pm 17$ Ma, $2,535 \pm 18$), Rhyacian ($2,184 \pm 23$, $2,079 \pm 21$ Ma), Orosirian ($2,000 \pm 20$ Ma, $1,969 \pm 18$ Ma, $1,875 \pm 20$), and Stenian ($1,119 \pm 24$ Ma) ages. The Meso-proterozoic zircon crystals are mainly rounded (75 %), more rarely sub-rounded (25 %) (Fig. 13).

With the exception of one Tonian date (898 ± 10 Ma), the Neo-proterozoic dates are Cryogenian (six grains) and Ediacaran (18 grains). The Cryogenian dates range from 790 ± 8 to 668 ± 7 Ma. The Tonian and Cryogenian zircon

crystals are mainly rounded (72 %), with only a few sub-rounded (14 %) and euhedral (14 %) grains. The Ediacaran zircon crystals are mainly euhedral (78 %), rarely rounded (16 %), or sub-rounded (6 %) (Fig. 13). Their sizes vary from 4.2Φ ($54.3 \mu\text{m}$ ESD) to 2.39Φ ($190 \mu\text{m}$ ESD). The ages range from 632 ± 7 Ma down to 544 ± 6 Ma. Three Ediacaran populations can be identified: one from 632 ± 7 Ma down to 616 ± 7 Ma ($N = 3$), one from 602 ± 7 Ma down to 590 ± 7 Ma ($N = 4$), and the last one from 576 ± 6 Ma down to 544 ± 6 Ma ($N = 11$), respectively.

The youngest group of mafic magmatic zircon grains comprises eight Ordovician grains, dominated by euhedral shape (88 %) and with size varying from 3.54Φ ($86.2 \mu\text{m}$) to 2.99Φ ($126 \mu\text{m}$). Their $^{206}\text{Pb}/^{238}\text{U}$ ages range from 487 ± 6 Ma down to 454 ± 5 Ma, with a mean age of 469 ± 10 Ma.

Metamorphic data are mainly associated with rims and overgrowths (68 %) with the exception of a few

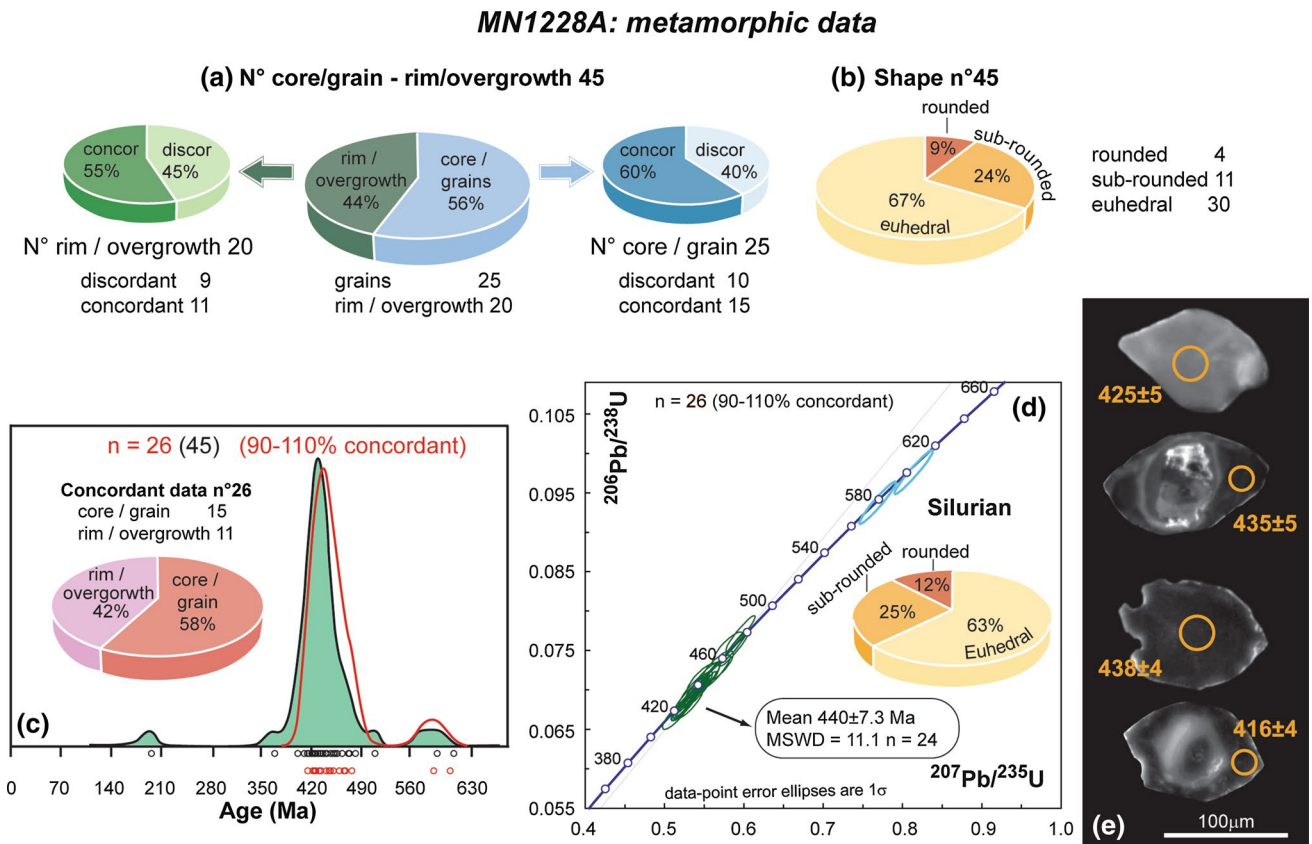


Fig. 11 Main characteristics of the metamorphic zircon grains of sample MN1228A (polygenic meta-sedimentary formation) from the Money Complex. **a** Pie charts comparing the amount of core/grain versus rim/overgrowth; concordant versus discordant dates in the rim/overgrowth group and in the core/grain group, respectively. **b** Pie chart comparing euhedral versus sub-rounded versus rounded zircon grains. **c** Kernel density estimate for all metamorphic grain ages (indicated by black circles in the upper row). Red line is kernel density estimate calculated for grain ages <10 % discordance (red circles in the lower row are single grain ages). Single-spot analyses

are given $^{206}\text{Pb}/^{238}\text{U}$ ages for results <1 Ga. Pie chart comparing the amount of core/grain versus rim/overgrowth for the concordant dates. **d** Zircon U-Pb Concordia plot for the Ediacaran and Silurian metamorphic 90–110 % concordant dates. Pie chart compares the amount of euhedral versus sub-rounded versus rounded Silurian zircon grains. **e** Cathodoluminescence (CL) images of representative metamorphic zircon crystals. Analysed spots are indicated by circles (diameter: 40 and 25 μm). Numbers indicate measured $^{206}\text{Pb}/^{238}\text{U}$ (<1 Ga) ages, with 1σ error

homogenous grains (32 %) (Fig. 14). Metamorphic grains are slightly rounded (32 %) and rounded (42 %), except for about 21 % of them that are euhedral. Only five of the 19 metamorphic grains yielded concordant dates, which are Cambrian to Ordovician in age, ranging from 494 ± 6 Ma to 453 ± 5 Ma. Most of the discordant dates are associated with rims and overgrowths, suggesting that the reason for discordance is the growth zoning or the growth of new zircon around old cores.

Discussion of the U-Pb results

Summary of the U-Pb results

Detrital zircon grains from the *Polygenic meta-sedimentary formation* (sample MN1228A) are dominantly pink

in colour. Taking into account all the concordant and discordant data, two well-defined groups have been identified at 650–550 and 450–400 Ma, respectively, whereas a third group comprises ages distributed over a large span (2,550–1,500 Ma). Zircon crystals were mainly derived from metamorphic sources and, to a lesser extent, from mafic magmatic sources. The analysis of the metamorphic concordant data shows the occurrence of two Ediacaran grains at 600 ± 7 Ma and 577 ± 6 Ma, respectively, and of a Silurian population. The latter comprises 24, mainly euhedral zircon grains with a mean concordia age of 440 ± 7 Ma. The ages of the mafic magmatic zircon grains range from $2,539 \pm 11$ Ma down to 438 ± 5 Ma. A main Cryogenian population has also been identified: It comprises six mostly euhedral grains with ages ranging from 743 ± 8 down to 638 ± 7 Ma.

Detrital zircon grains from the *Monogenic meta-sedimentary formation* (sample MN1202A) are mostly

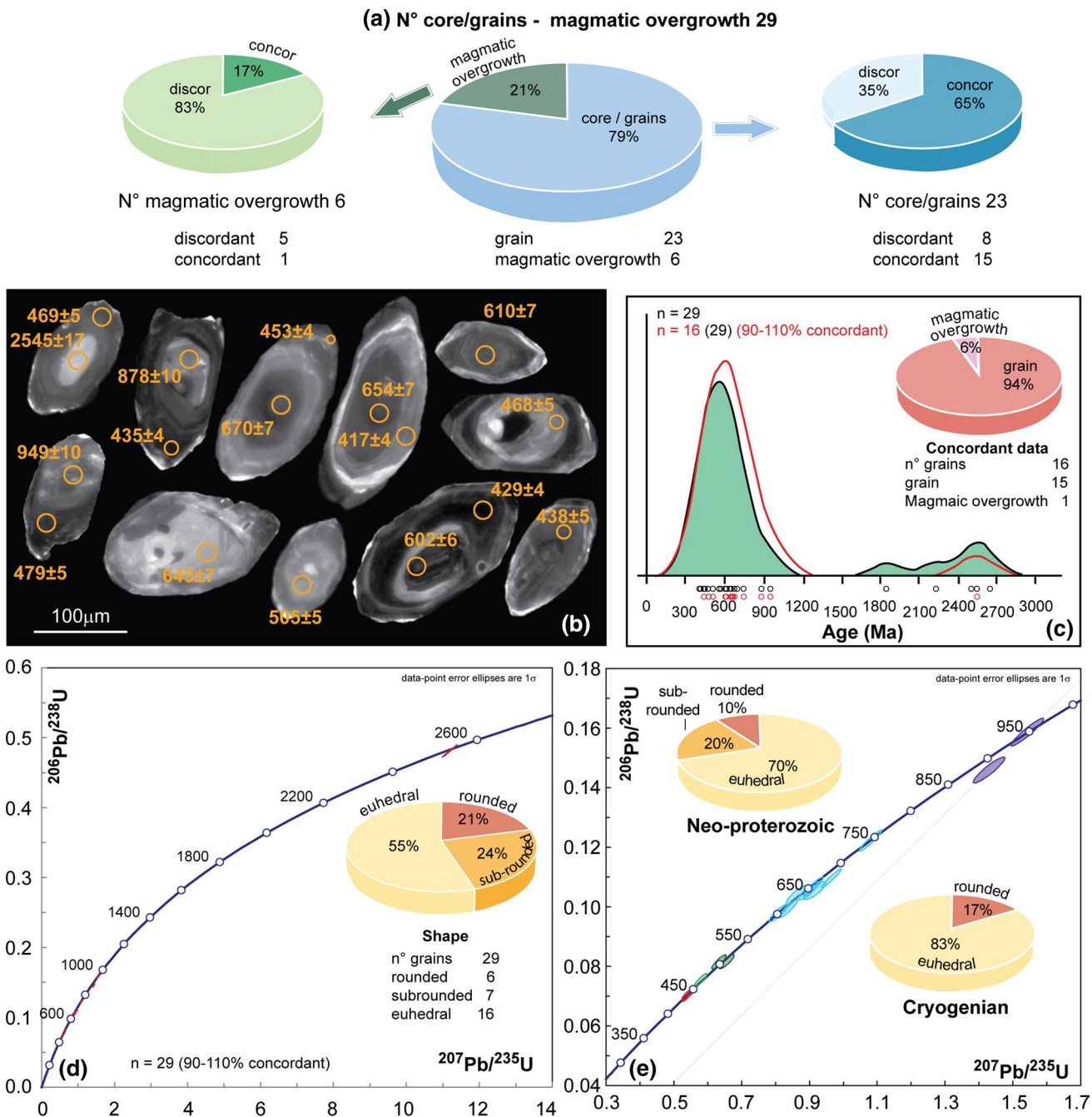
MN1228A: magmatic data

Fig. 12 Main characteristics of the magmatic zircon grains of sample MN1228A (polygenetic meta-sedimentary formation) from the Money Complex. **a** Pie charts comparing the amount of core/grain versus magmatic overgrowth; concordant versus discordant dates in the magmatic overgrowth group and in the core/grain group, respectively. **b** Cathodoluminescence (CL) images of representative magmatic zircon crystals. Analysed spots are indicated by circles (diameter: 40 and 25 μm). Numbers indicate measured $^{207}\text{Pb}/^{206}\text{Pb}$ (>1 Ga) $^{206}\text{Pb}/^{238}\text{U}$ (<1 Ga) ages, with 1σ error. **c** Kernel density estimate for all magmatic grain ages (indicated by black circles in the upper row). Red line is kernel density calculated for grain ages $<10\%$. **d** Zircon U-Pb Concordia plot for the magmatic 90–110 % concordant dates. Pie chart compares the amount of euhedral versus sub-rounded versus rounded magmatic zircon grains. **e** Zircon U-Pb Concordia plot for the magmatic Neo-proterozoic and Palaeozoic 90–110 % concordant dates. Pie charts compare the amount of euhedral versus sub-rounded versus rounded zircon grains in all the Neoproterozoic group and in the Cryogenian subgroup

discordance (red circles in the lower row are single grain ages). Single-spot analyses are given as $^{206}\text{Pb}/^{238}\text{U}$ ages for results <1 Ga. Pie chart comparing the amount of core/grain versus magmatic overgrowth in the concordant dates. **d** Zircon U-Pb Concordia plot for the magmatic 90–110 % concordant dates. Pie chart compares the amount of euhedral versus sub-rounded versus rounded magmatic zircon grains. **e** Zircon U-Pb Concordia plot for the magmatic Neo-proterozoic and Palaeozoic 90–110 % concordant dates. Pie charts compare the amount of euhedral versus sub-rounded versus rounded zircon grains in all the Neoproterozoic group and in the Cryogenian subgroup

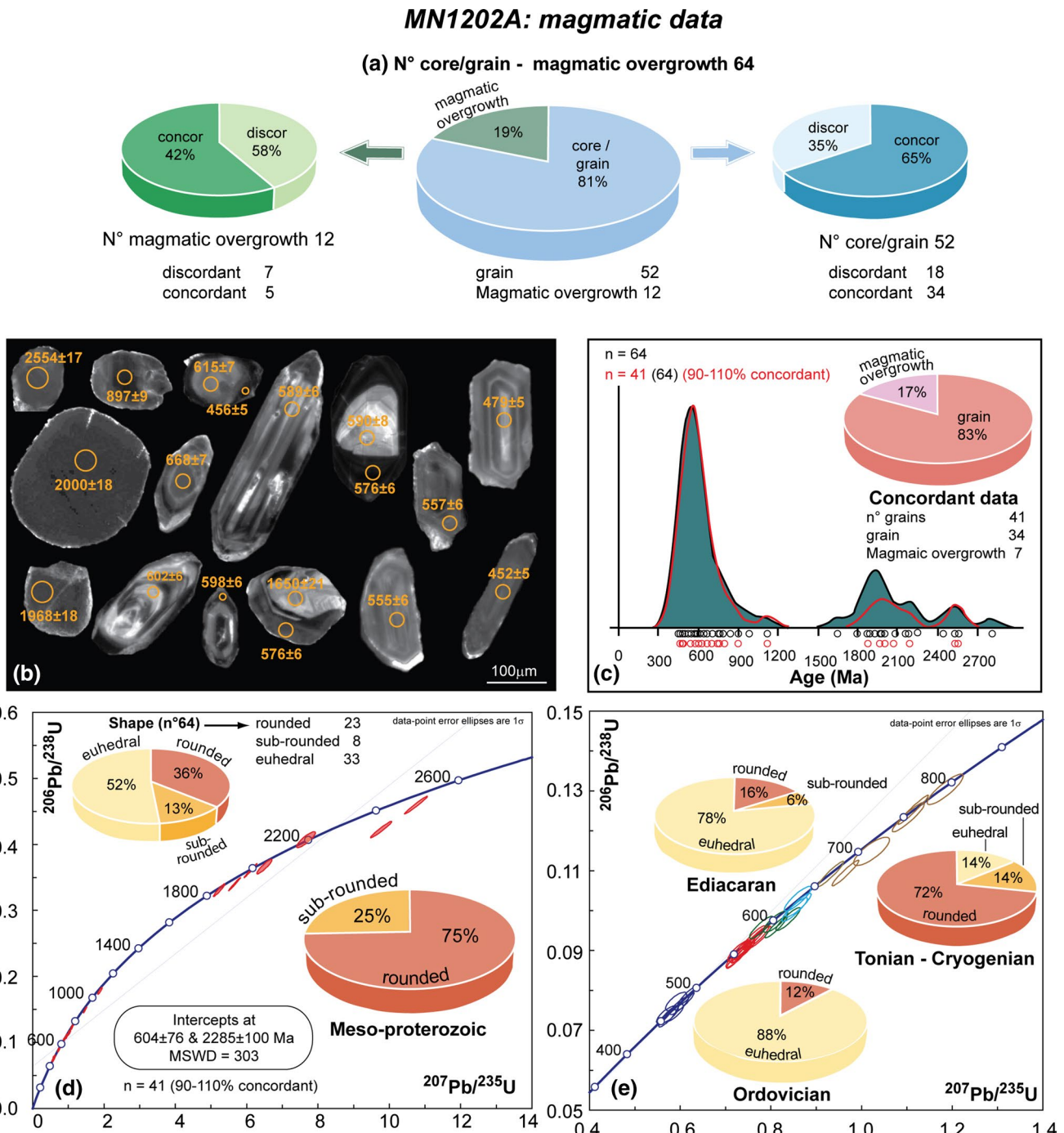


Fig. 13 Main characteristics of the magmatic zircon grains of sample MN1202A (monogenic meta-sedimentary formation) from the Money Complex. **a** Pie charts comparing the amount of core/grain versus magmatic overgrowth; concordant versus discordant dates in the magmatic overgrowth group and in the core/grain group, respectively. **b** Cathodoluminescence (CL) images of representative magmatic zircon crystals. Analysed spots are indicated by circles (diameter: 40, 30, 25, and 16 μm). Numbers indicate measured $^{207}\text{Pb}/^{206}\text{Pb}$ (≥ 1 Ga) and $^{206}\text{Pb}/^{238}\text{U}$ (< 1 Ga) ages, with 1σ error. **c** Kernel density estimate for all magmatic grain ages (indicated by black circles in the upper row). Red line is kernel density estimate calculated for grain ages $< 10\%$ discordance (red circles in the lower row are single grain

ages). Single-spot analyses are given as $^{207}\text{Pb}/^{206}\text{Pb}$ ages for results ≥ 1 Ga and $^{206}\text{Pb}/^{238}\text{U}$ ages for results < 1 Ga. Pie chart comparing the amount of core/grain versus magmatic overgrowth in the concordant data. **d** Zircon U-Pb Concordia plot for the magmatic 90–110 % concordant dates. Pie chart compares the amount of euhedral versus sub-rounded versus rounded magmatic zircon grains with respect to all the analysed crystals and to the Meso-Proterozoic grains. **e** Zircon U-Pb Concordia plot for the magmatic Cryogenian to Ordovician 90–110 % concordant dates. Pie charts compare the amount of euhedral versus sub-rounded versus rounded zircon grains in the Tonian-Cryogenian, Ediacaran and Ordovician zircon grains, respectively

MN1202A: metamorphic data

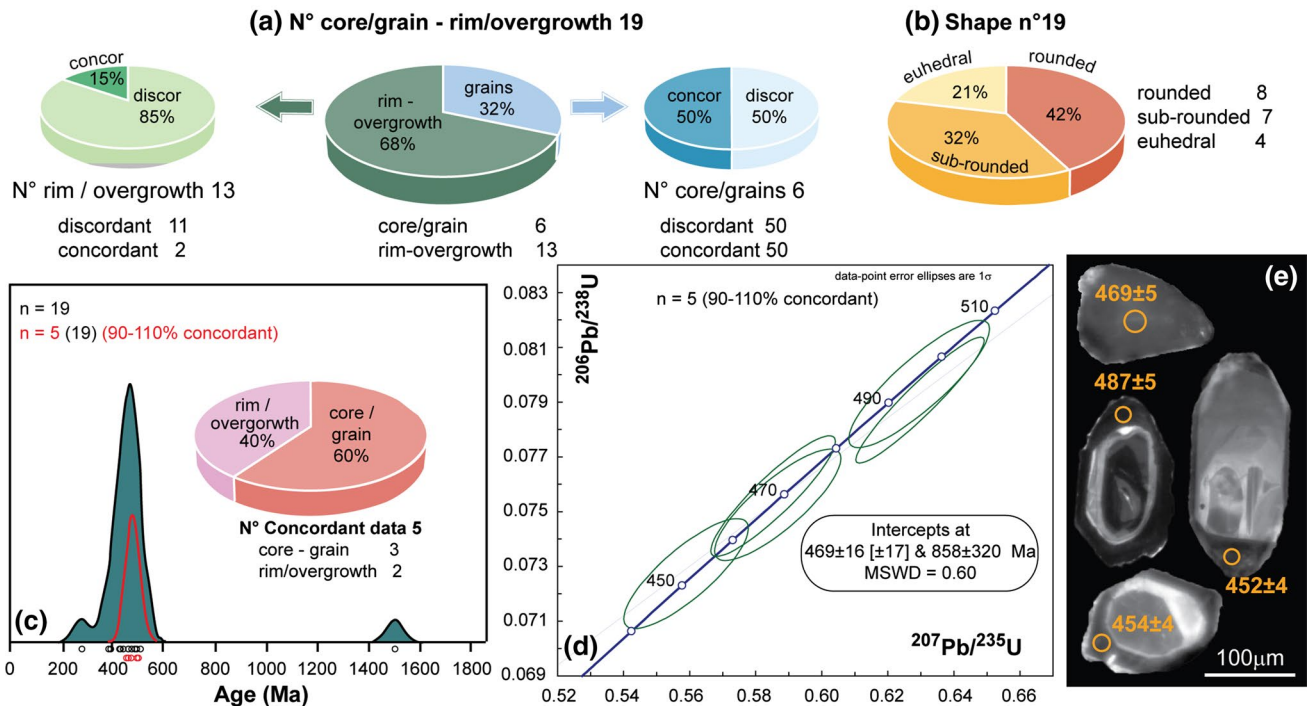


Fig. 14 Main characteristics of the metamorphic zircon grains of sample MN1202A (monogenic meta-sedimentary formation) from the Money Complex. **a** Pie charts comparing the amount of core/grain versus rim/overgrowth; concordant versus discordant dates in the rim/overgrowth group and in the core/grain group, respectively. **b** Pie chart comparing euhedral versus sub-rounded versus rounded zircon grains. **c** Kernel density estimate for all metamorphic grain ages (indicated by black circles in the upper row). Red line is kernel density estimate calculated for grain ages <10 % discordance (red circles).

cles in the lower row are single grain ages). Single-spot analyses are given as $^{207}\text{Pb}/^{206}\text{Pb}$ ages for results ≥ 1 Ga and $^{206}\text{Pb}/^{238}\text{U}$ ages for results <1 Ga. Pie chart comparing the amount of core/grain versus rim/overgrowth for the concordant dates. **d** Zircon U-Pb Concordia plot for the Ordovician and Cambrian metamorphic 90–110 % concordant dates. **e** Cathodoluminescence (CL) images of representative metamorphic zircon crystals. Analysed spots are indicated by circles (diameter: 25 and 16 μm). Numbers indicate measured $^{207}\text{Pb}/^{206}\text{Pb}$ (≥ 1 Ga) and $^{206}\text{Pb}/^{238}\text{U}(<1$ Ga) ages, with 1σ error

colourless, and only rarely pink. With respect to the polygenetic meta-sedimentary formation, a higher percentage of them is sub-rounded or rounded in shape. Two main age clusters have been recognized at 450–400 Ma and 650–500 Ma, respectively. Older ages, spanning between 2,720–1,000 Ma, form a less well-defined group. Zircon crystals mainly derive from mafic magmatic sources and, to a lesser extent, from metamorphic sources. The concordant mafic dates range from $2,720 \pm 12$ Ma down to 454 ± 5 Ma. Three main concordant age groups have been recognized. The first one comprises mostly rounded zircons with ages ranging from 790 ± 8 Ma down to 668 ± 7 Ma (i.e. Cryogenian). The second population comprises Ediacaran, mainly euhedral zircon crystals with ages ranging from 632 ± 7 Ma down to 544 ± 6 Ma. A more detailed subdivision allowed to distinguish three different Ediacaran groups (i) from 632 ± 7 Ma to 616 ± 7 Ma, (ii) from 602 ± 7 Ma to 590 ± 7 Ma, and (iii) from 576 ± 6 Ma to 544 ± 6 Ma. The third main concordant U-Pb group comprises euhedral mafic zircons with ages ranging from

487 ± 6 Ma to 454 ± 5 Ma (i.e. Ordovician). The metamorphic zircon grains are mainly sub-rounded or rounded, and only few grains yielded concordant dates which are Cambrian to Ordovician in age, ranging from 494 ± 6 Ma to 453 ± 5 Ma.

In both samples (MN1228A and MN1202A), the analysis of zircon grains show that the amount of rounded grains increases with their age. This suggests that there is a relationship between the roundness of zircon grains and their polycyclic origin, as shown by Malusà et al. (2013) in modern sands shed from the Alps.

Constraints on the maximum age of sedimentation of the Money Complex

The detrital zircon ages, combined with the lithostratigraphic data, allow to define the maximum deposition age of the whole sequence outcropping in the Money window. Indisputably, this sequence comprises post-Silurian sediments because the youngest detrital zircon grains in the two

samples yield concordant $^{206}\text{Pb}/^{238}\text{U}$ dates of 407 ± 5 Ma (MN1228A, polygenic meta-sedimentary formation) and 439 ± 5 Ma (MN1202A, monogenic meta-sedimentary formation), which correspond Silurian to Lower Devonian ages, respectively. Although there is no evidence for Carboniferous detrital zircon grains, it may be argued that the whole sequence was deposited during the late Carboniferous-early Permian. Several arguments support this interpretation, specifically (i) the lack of pre-Alpine, high-temperature mineral relics, (ii) the presence of graphite, and (iii) the occurrence of conglomeratic levels interlayered within the graphite-bearing micaschists. Each of these arguments will be briefly discussed below.

The lack of pre-Alpine, high-temperature mineral relics in the Money Complex could result either from the absence of high-temperature metamorphism during the pre-Alpine history or from the lack of preservation as a consequence of an intense reworking during the Alpine history. However, we note that pre-Alpine garnet relics have been found close to the contact between the monogenic sedimentary formation and the Erfauft meta-granite, where they are interpreted as linked to the contact metamorphism associated with the intrusion of the Erfauft granite (Le Bayon and Ballèvre 2004). Moreover, multi-stage garnets have been found away from the contact with the Erfauft meta-granite, but a careful analysis revealed that they are made of detrital cores surrounded by Alpine overgrowths (Manzotti and Ballèvre 2013). If a pre-Alpine metamorphism in the garnet stability field was present in the Money Complex, our studies should have been able to identify it. According to these observations, we consider that a pre-Alpine, high-temperature metamorphism (amphibolite to granulite-facies conditions) is lacking in the studied sequence.

The presence of carbonaceous material in a sedimentary sequence is not a sufficient criterion to argue for a late Carboniferous-early Permian age for the sedimentation. Organic-rich sequences in Palaeozoic sediments are in fact by no means restricted to the Carboniferous. Outside the Alpine belt, Ordovician and Silurian carbonaceous-rich sediments are well known in pre-orogenic, marine deposits (Servais et al. 2008; Verniers et al. 2008). In the Alpine belt, Ordovician and Silurian carbonaceous-rich sediments have been described in the Austroalpine and Southalpine units (Schönlau 1992; Neubauer and Sassi 1993). The graphite-bearing schists from the internal Briançonnais nappes (to the west of the studied area) were initially thought to be Carboniferous in age (Ellenberger 1958, 1966). However, on the basis of Cambro-Ordovician ages obtained for magmatic bodies intruded into these sediments (Guillot et al. 1991), it has been subsequently demonstrated that the graphite-bearing schists belong to an early Palaeozoic sequence.

However, the presence of conglomeratic levels interlayered with carbonaceous-rich sediments is a key lithological character that can be used to recognize Carboniferous sequences, deposited in a continental (fluvial or lacustrine) environment (McCann et al. 2008; Opluštil et al. 2013). Therefore, the polygenic sedimentary formation of the Money Complex bears much more similarities with late Carboniferous syn-orogenic sequences deposited in intramontane basins (e.g. Franz et al. 1991; Krainer 1993; Pestal et al. 1999; Capuzzo and Wetzel 2004; Veselà and Lammerer 2008) rather than with the pre-orogenic, marine, early Palaeozoic deposits. Moreover, layers with lenticular shape, interpreted as channel deposits, occur in both the polygenic and monogenic meta-sedimentary formations (see section “Depositional setting”), suggesting that the Money Complex was probably deposited in a continental fluvial system late Carboniferous in age.

We therefore conclude that the Money Complex was most probably deposited during the late Carboniferous, but that the drainage area (considering the fact that no sampling bias was made during the picking of the grains) that provided the detrital material did not contain exposed Carboniferous zircon-bearing rocks. This result is rather unexpected, given the huge amount of Carboniferous granites all over the Variscan belt (Finger et al. 1997), most of which intruded the basement during the deposition of the coal-bearing basins, and their volcanic counterparts being associated to explosive, distal ejecta within the coal-bearing sequences (the famous “tonsteins”) (Königer et al. 2002). The lack of detrital zircons of Carboniferous age requires therefore a careful discussion of the potential sources for the Money Complex.

Identification of the source areas for the Money Complex

A synthesis of the available geochronological data for the Western and Central Alps (Fig. 15 and Supplementary data Tables 4–8 and Fig. 1) is used to discuss and to identify the possible source areas for the Money Complex.

Few *Cambrian to Ediacaran* magmatic ages have been obtained in detrital grains from the two meta-sedimentary formations. Cambrian to Ediacaran magmatic events have been dated in the basement rocks of the External Massifs (e.g. Ménot et al. 1988), in the Briançonnais Zone in the Western Alps (e.g. Guillot et al. 1991; Bertrand et al. 2000b; Scheiber et al. 2014), and in the Central Alps (Schaltegger et al. 2002; Vonlanthen et al. 2012; see Fig. 15 and Supplementary data Table 4 and Fig. 1 for complete references).

In both the polygenic and monogenic meta-sedimentary formations of the Money Complex, detrital zircon geochronology points to an *Ordovician magmatism*. Ordovician magmatism has been dated in the External Massifs (e.g. Oberli et al. 1994; Abrecht et al. 1995; Rubatto et al. 2001)

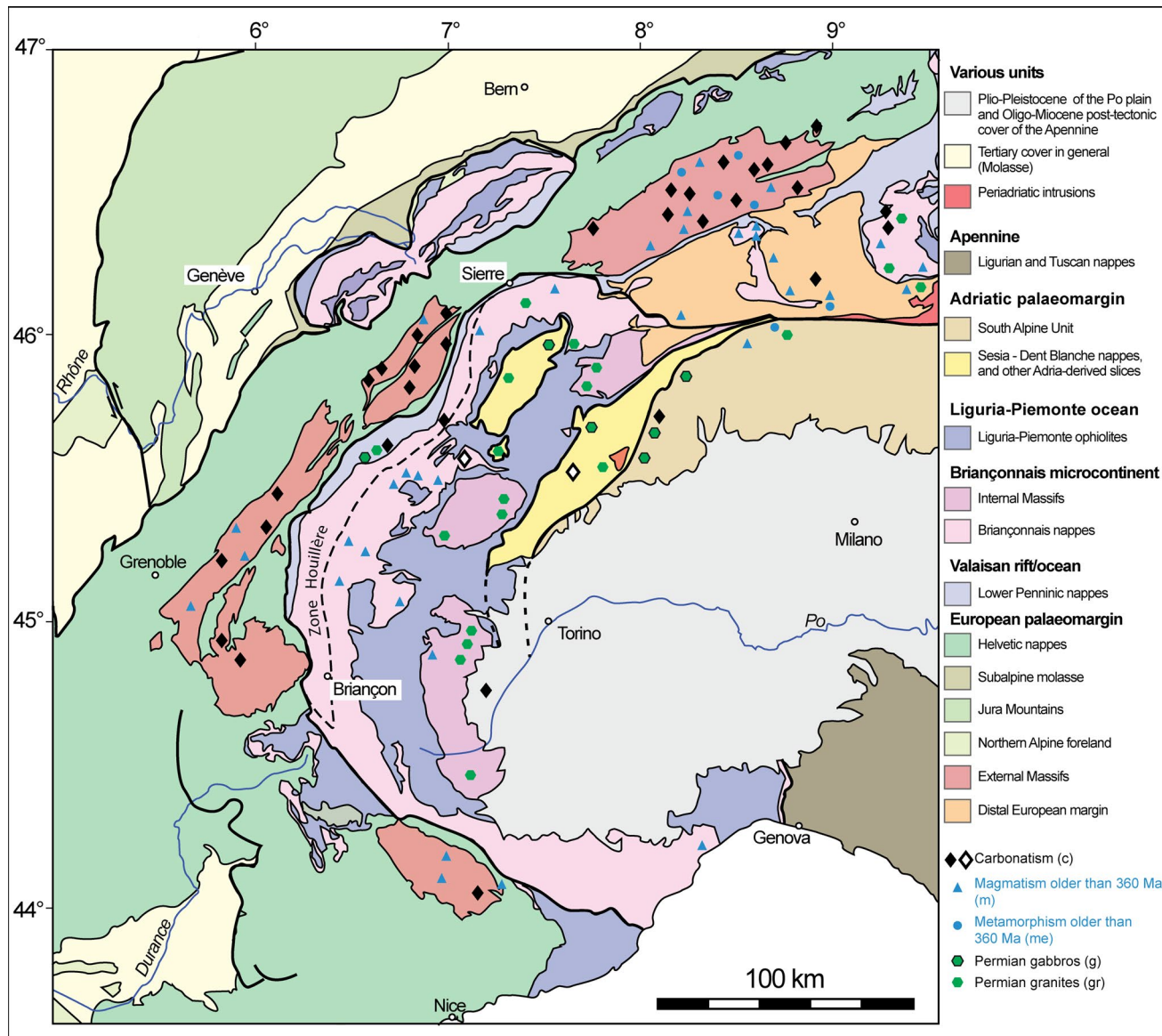


Fig. 15 Tectonic map of the Western Alps with the distribution of (i) Carboniferous magmatism (black and white diamonds), (ii) Magmatism older than 360 Ma (blue triangles), (iii) Metamorphism older than 360 Ma (blue circles), and (iv) Permian magmatism (green hexagons). See supplementary data Tables 4–8 and Fig. 1 for a detailed description of the main characteristics, ages, and references of the reported magmatic and metamorphic rocks. The dashed black line delimits the Zone Houillère

ages). See supplementary data Tables 4–8 and Fig. 1 for a detailed description of the main characteristics, ages, and references of the reported magmatic and metamorphic rocks. The dashed black line delimits the Zone Houillère

and in the distal European margin (e.g. Steiger et al. 1994; Vonlanthen et al. 2012), in the Briançonnais basement (e.g. Bertrand and Leterrier 1997; Guillot et al. 2002), as well as in the Southalpine basement (Köppel and Grünfelder 1971; see Fig. 15; Supplementary data Table 4 and Fig. 1 for complete references).

In the Sapey gneiss (Briançonnais basement), the Ordovician magmatic zircon grains frequently display inherited cores at 2,400, 720 Ma and at ca. 600–650 Ma, respectively, and a regularly zoned outer rim (Péclet orthogneiss and Modane porphyritic granite, Bertrand et al. 2000b). Similar types of zircon grains (in terms of textures and

ages) have been found in both samples from the Money Complex (Figs. 12b, 13b).

In both meta-sedimentary formations from the Money Complex, some detrital zircons record pre-Carboniferous metamorphism. Silurian ages have been found in detrital grains from the polygenic meta-sedimentary formation, whereas the monogenic meta-sedimentary formation provided Cambrian and Ordovician ages. Rare and often poorly constrained pre-Carboniferous metamorphic ages have been found in the basement rocks of the External Massifs (e.g. Gebauer et al. 1988), in the Central Alps (Vonlanthen et al. 2012) and in the Southalpine unit (Franz

and Romer 2007; see Fig. 15; Supplementary data Table 5 and Fig. 1 for complete references).

In the Eastern Alps, a Lower Ordovician high-grade metamorphism has been dated in the Ötztal crystalline basement (Klötzli-Chowanetz et al. 1997). In the basement of the Briançonnais (Western Alps) (Gaggero et al. 2004), and in other parts of the Alps (Boriani et al. 2003 and refs therein), a pre-Carboniferous metamorphism has been suggested only on the basis of the Ordovician ages obtained for the granite intrusions. Regrettably, specific geochronological data that clearly confirm this metamorphic event are still largely missing. Therefore, although this is still a matter of debate, what is clear is that during the Cambro-Ordovician time, crustal melting produced a large amounts of acidic melts, as demonstrated by the plutonic bodies and volcanic products recognized over a very large area (Western and Eastern Alps) (Hoinkes and Thöni 1993 and refs therein; Gaggero et al. 2004). This magmatic event was probably accompanied or preceded by a regional metamorphism, the extent and the degree of which remain not well established (e.g. Raumer et al. 2012).

Unexpectedly, no Carboniferous zircon grains have been found in the analysed samples from the Money Complex. However, *Carboniferous magmatism* is widespread in the External Massifs, with mafic intrusives and more evolved types (e.g. Oberli et al. 1981; Schaltegger and Corfu 1992; Sergeev and Steiger 1993; Bussy et al. 1998a, 2000a; Guerrot and Debon 2000; Rubatto et al. 2001) (Fig. 15; Supplementary data Table 6 and Fig. 1 for references). This magmatic episode has been interpreted as the consequence of the post-collisional readjustment of the thickened Variscan continental lithosphere (Schaltegger and Corfu 1992; Bonin et al. 1993; Bussy et al. 2000a). In the internal Alps, evidence for a Carboniferous magmatism is rare and sparse, being only known in very few occurrences in the Briançonnais (Bussy and Cadoppi 1996; Bertrand et al. 1998, 2000a; Scheiber et al. 2013), in the Austroalpine, and in the Southalpine unit (Rubatto and Gebauer 1997; Rubatto et al. 1999).

As expected, Permian detrital zircons are not present in the studied samples from the Money Complex. *Permian magmatism* is well known in many parts of the Alps (e.g. Thöni and Jagoutz 1992; Thöni et al. 1992; Visonà 1995; Miller and Thöni 1997; Visonà 1997; Bussy et al. 1998b; Vavra et al. 1999; Monjoie et al. 2005; Peressini et al. 2007; Schaltegger and Brack 2007; Beltrando et al. 2010; Cenki-Tok et al. 2011) (Fig. 15; Supplementary data Table 7 and 8 and Fig. 1 for references). The Permian magmatism was associated with a high-temperature metamorphism (Lardeaux and Spalla 1991; Abrecht et al. 1995; Vavra et al. 1999; Hermann and Rubatto 2003; Peressini et al. 2007; Manzotti et al. 2012; Ewing et al. 2013).

Therefore, the absence of Carboniferous and Permian detrital zircons and the presence of Cambro-Ordovician

detrital ones suggest that the basement units now forming the Briançonnais microcontinent represent the potential sediment sources for the polygenic and monogenic formations from the Money Complex.

Implications for the late Carboniferous-early Permian palaeogeography

Late Carboniferous history of the European palaeomargin

During the *late Carboniferous*, southern Europe was dominated by the orogenic then post-orogenic evolution of the Variscan belt. The post-collisional readjustment of the thickened Variscan crust produced a diffuse magmatic activity, which is widespread in the External Zone of the Alpine belt (i.e. External Massifs; Schaltegger and von Quadt 1990; Schaltegger and Corfu 1992; Sergeev and Steiger 1993; Bussy and von Raumer 1994; Schaltegger and Corfu 1995; Bussy et al. 2000b; Guerrot and Debon 2000; Rubatto and Hermann 2001) (Fig. 15; Supplementary data Table 6 and Fig. 1). Crustal extension associated with fast exhumation (Ménard and Molnar 1988) resulted in the opening of several rapidly subsiding, intramontane basins, like the Salvan-Dorénaz basin (Niklaus and Wetzel 1996; Capuzzo et al. 2003; Capuzzo and Wetzel 2004), the La Mure (Gignoux and Moret 1952; Haudour 1976), the Clue de Verdaches-Barles (Greber 1965; Guiomar 1989), and the Argentera (Corsin and Faure-Muret 1946; Faure-Muret 1955). Most of these basins are elongated parallel to the SW-NE Variscan strike and were bordered by syn-sedimentary faults (Krainer 1993; Cassinis et al. 1995). The temperate wet climate allowed for the accumulation of organic matter and the formation of coal seams. Coarse-grained clasts of fluvial origin and fine lacustrine sediments, delivered from high-relief areas, were trapped in these basins. Widespread intrusive and extrusive magmatic rocks of both mantle and crustal origins also contributed to their infillings (von Raumer 1993; Cortesogno et al. 1998; Capuzzo and Bussy 2000). This sedimentary cycle, which persisted from the late Carboniferous (mostly Upper Pennsylvanian) down to the early Permian, is found all over the Variscan belt from the Armorican Massif to the Bohemian Massif, and, within the Alpine belt, is characteristic of the External Massifs (Gignoux and Moret 1952; Faure-Muret 1955; Capuzzo and Wetzel 2004).

Late Carboniferous history of the Briançonnais microcontinent

The Zone Houillère in the Briançonnais microcontinent (Fabre et al. 1982; Mercier and Beaudoin 1984, 1987) presents a different history, firstly because the sedimentation

had a long-lasting history, from the Upper Mississippian to Upper Pennsylvanian, and because a late Carboniferous magmatism is lacking in both the basement of the basin and in the basin itself. The Zone Houillère was an elongated, narrow basin, extending today over an area of 1,000 km², from Briançon to the south to the Valais to the north, and occurring in most of the frontal part of the Briançonnais nappes. The Zone Houillère comprises a Carboniferous (mainly Upper to Middle Pennsylvanian, Greber 1965; Brousse Delcambre et al. 1995, 1997) and Permian sequence of continental deposits, overlain by Lower Triassic quartzite and then Middle and Upper Triassic carbonates (Ellenberger 1958; Fabre 1961; Fabre et al. 1982; Mercier and Beaudoin 1984, 1987). The Carboniferous detrital sequence reaches a thickness of about 2,500 m (Fabre 1961; Feys 1963). Even if the stratigraphy and the age of the Zone Houillère are reasonably well known, on the contrary, the origin and the tectonics associated with this wide sedimentary basin still remain unknown.

Two mega-sequences have been distinguished in the Zone Houillère. In the lower mega-sequence, palaeocurrent studies indicate the presence of a south-south-west to north-north-east drainage pattern, active from Lower to Middle Pennsylvanian (Mercier and Beaudoin 1987). Braided systems were present in the southern part of the basin, whereas lacustrine deposits developed more towards the north (Fig. 16). The basement rocks of the recent Pelvoux, Belledonne, and Argentera External Massifs may have been potential source area for the clastic sediments of the Zone Houillère. In the upper mega-sequence (Upper Pennsylvanian), deposition started also in the north part of the basin, as result of a period of intense subsidence. In this northern region of the basin, the main drainage pattern was developed from south-south-east to north-north-west and was dominated by both braided and meandering systems (Mercier and Beaudoin 1987). Therefore, according to the main palaeocurrent directions, the potential source areas for this northern region may be represented by basement portions located to the east (in its present position) of the Zone Houillère basin, which were probably similar to the ones now forming the Briançonnais microcontinent. Probably, in this northern region of the basin, continental clasts provided by the External Massifs of the Alpine belt could not be present for drainage reasons. Therefore, the late Carboniferous evolution recorded in the Money Unit is fully consistent with the fact that it belonged to the Briançonnais microcontinent, and that it had no link with the External Massifs.

It has to be noted that only very few evidence for a late Carboniferous magmatism or metamorphism has been found up to now in the Briançonnais microcontinent. A complete crustal section of the Briançonnais microcontinent is not known. However, some inferences can be made

regarding its Carboniferous evolution. Firstly, the lack of Carboniferous granites indicates that no significant partial melting took place in the lower crust, as depicted in Fig. 16a, in contrast with the basement of the External Zone. Secondly, in the middle to upper crust of the Briançonnais basement, the metamorphic grade was significantly lower compared with the External Massifs, where migmatites were produced and exhumed during the Carboniferous. Therefore, the Briançonnais basement records a different tectonic evolution compared with the External Massifs.

Early Permian history

In south-western Europe, the *Carboniferous-Permian boundary* marked the beginning of a different geodynamic regime, during which the plate convergence gave way to a transtensional strike-slip tectonics (Ziegler 1993; Marotta and Spalla 2007; Schuster and Stüwe 2008; Spalla et al. 2014). The western collisional Variscan margin between Gondwana and Laurasia progressively became a diffuse dextral transform margin (Cassinis et al. 2012). The progressive transformation of the Western Variscan chain from a collisional to a dextral shear margin has been connected with the beginning of the north-directed subduction of the Palaeotethys oceanic ridge beneath Eurasia and the already-formed Variscan chain (Gutiérrez-Alonso et al. 2008). During Lower Permian, the Variscan relief was not higher than ca 2 km (Fluteau et al. 2001) and was progressively and completely peneplanated during the Upper Permian (Cassinis et al. 2012). The transition between the Carboniferous and Permian times (Upper Pennsylvanian to the beginning of the Permian) was also characterized by climate changes, from humid to moderately semi-arid conditions (Dal Cin 1972; Krainer 1993), with the alternation of wet and dry periods (Roscher and Schneider 2006). In south-western Europe, the tectonic evolution is well recorded by peculiar structural, sedimentary, metamorphic, and magmatic signatures. The transtensional to strike-slip tectonic movements were responsible for the opening of a great number of subsiding basins (Fig. 1; Supplementary data Table 1 and Fig. 1) (Arthaud and Matte. 1977; Cassinis and Perotti 2007; Gretter et al. 2013), which are generally considered as pull-apart continental troughs. In the central part of the Southalpine unit, early Permian strike-slip tectonics was mainly concentrated along both the palaeo-Giudicarie and Insubric faults and have generated asymmetric graben basins (e.g. Orobic Basin, Collio Basin, Tregiovo-Mt. Luco Basins) (Matte 1986; Massari 1988; Cassinis et al. 1995). These basins were mostly filled with continental deposits (derived from magmatic and siliciclastic rocks) and only subordinate marine deposits (i.e. Bellerophon Formation in the Adige Valley and Pontebba Supergroup in the Carnic Alps). Volcanic rocks

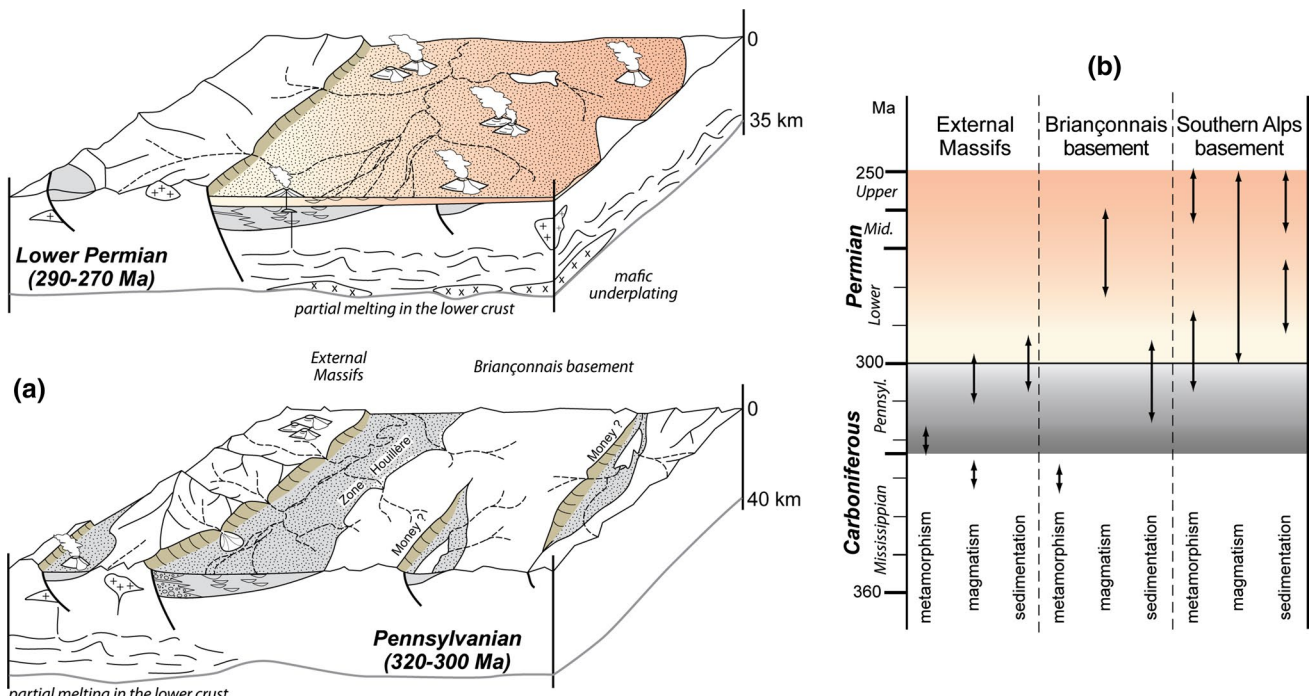


Fig. 16 **a** Simplified palaeoenvironmental-depositional scenarios from late Carboniferous to early Permian time, compiled for the Western Alps. **b** Table that summarizes the main metamorphic, mag-

matic, and sedimentary signals in the External Massifs and in the basement of the Briançonnais microcontinent and Southern Alps

(ignimbrites, tuffs, and lava flows) show a calc-alkaline acidic-to-intermediate composition. The continental sediments mainly formed fluvio-lacustrine and locally fluvio-palustrine deposits (Cassinis et al. 2012). The Permian arid to semi-arid climate resulted in the silicate weathering, hence the red colour of the Permian sediments, and in the oxidation of the organic matter, hence the gradual disappearance of the carbonaceous material.

In the Southalpine domain, a subsequent well-differentiated tectono-sedimentary cycle, devoid of any volcanic activity, has been recognized in the late Permian to the early Middle Triassic succession (Cassinis et al. 1988; Massari et al. 1994). This cycle has been considered to reflect the Middle-Upper Permian opening of the Neotethys Ocean with the onset of a generalized extensional tectonic regime and the progressive westward marine ingression (Cassinis et al. 2012). Moreover, this evolution has been related to the transition from a dextral shear to an extensional tectonic regime.

The Permian evolution is also recorded by magmatism and metamorphism. In the future Briançonnais microcontinent, Permian magmatism is found in the Zone Houillère (the sills and dykes of microdiorites that intrude the late Carboniferous sequence), and a Middle Permian granitic plutonism is widespread further east, in the Monte Rosa-Gran Paradiso-Dora-Maira nappes, i.e. in the Internal

Massifs. A widespread magmatic activity accompanied by a high-temperature metamorphism affected the Adriatic palaeomargin during the Permian times (Schuster et al. 2001; Spalla et al. 2014 and refs therein) (Fig. 15; Supplementary data Tables 7 and 8 and Fig. 1 for references). In the latter case, there is a clear genetic and temporal link between mantle melts accumulating at the base of the crust, partial melting in the lower crust, intrusion of granitic bodies at higher levels, and finally explosive, acid volcanism at the surface (e.g. Quick et al. 2009). The abundance of intermediate to felsic magmatism in the Zone Houillère and of granitoid intrusions in the Internal Massifs has the same implications, revealing that the lower crust from these areas was also melted during the Permian (Fig. 16b). On the contrary, these Permian magmatic and metamorphic signatures, which reflect a high-thermal regime, are not known in the External Massifs (Fig. 16b).

Several authors suggested that these magmatic and metamorphic signals cannot simply be the result of the thermal relaxation of the thickened lithosphere after the Variscan orogeny, associated with late orogenic extension. The high-thermal regime has been interpreted as the result of a hot asthenospheric mantle upwelling under the continental plate and of continental rifting (Diella et al. 1992; Müntener and Hermann 2001; Marotta and Spalla 2007; Schuster and Stüwe 2008).

Integration of the studied area at a larger scale

The lithological, petrographical, and stratigraphical data together with our U–Pb results suggest that the Money Complex records the late Carboniferous–early Permian evolution. The polygenic meta-sedimentary formation at the bottom of the sequence displays meta-conglomeratic layers interlayered with graphite-bearing micaschists (former organic-rich sandstones and mudstones). These continental fluvio-lacustrine sediments reflect the temperate wet climatic conditions that characterized the late Carboniferous. The biotite-amphibole-bearing orthogneiss may represent alkaline volcanics, whereas the albite-bearing paragneiss (meta-greywackes) with amphibolite layers may correspond to volcanic-rich clastic sediments and basalt lava flows, respectively. The beginning of the Permian and the climate change (from wet to semi-arid and arid conditions) are expected to be recorded by the sediments forming the monogenic meta-sedimentary formation (at the top of the sequence) that consists of quartz-pebble meta-conglomeratic layers intercalated with quartz-micaschists (former sandstones and siltstones) with rare occurrence of graphite layers. The quartz pebbles derive from the erosion of the Variscan relief, and the maturity of the conglomerates indicates a long-lasting transport potentially associated with an intense weathering of the source area. The rare occurrences of graphite can be related to the semi-arid conditions that did allow, only episodically, the preservation of a large amount of organic matter. Sedimentological similarities exist between the monogenic meta-sedimentary formation of the Money Complex and the Basal Conglomerate, the latter being deposited at the bottom of the Orobic Basin and ascribed to the early Permian (Cadel et al. 1996) (Fig. 1; Supplementary data Table 1). Finally, the Erfauft granite that intruded the monogenic meta-sedimentary formation of the Money Complex may be considered as a Permian laccolith.

Conclusion

The identification of the potential sources for the sediments forming the Money Complex has regional implications for the late Carboniferous–early Permian palaeogeography of the Alpine region, as summarized below.

1. The Money Unit (Money Complex + Erfauft granite), classically ascribed to the Briançonnais microcontinent (Compagnoni et al. 1974), crops out as a tectonic window below the overthrust Gran Paradiso Unit, and its present position is the result of the Alpine tectonic evolution.
2. Detrital zircon geochronology suggests that the sources for the sediments of the Money Complex could be

represented by basement portions similar to the ones belonging to the Briançonnais microcontinent. These basement slices display evidence for the Cambro-Ordovician magmatic and metamorphic evolution, but they did not record a significant Carboniferous and Permian magmatic and/or metamorphic activity.

3. The lack of Carboniferous detrital zircons in the Money Complex indicates that this sequence was deposited in an area where the sedimentary contributions from the External Massifs could not arrive. Therefore, it may be suggested that the Money Complex could have been deposited in the Zone Houillère itself, provided that it was located on its eastern margin. Alternatively, the Money Complex may represent a small late Carboniferous–Permian basin, located to the east of the depositional area of the Zone Houillère (Fig. 16).
4. The pre-Alpine basement of the Briançonnais microcontinent is characterized by the lack of a significant granitic magmatism of late Carboniferous age and by the widespread presence of granites, diorites, and volcanics Permian in age (Fig. 16). In addition, the age of its metamorphism is largely unknown, although it is generally assumed to be “Variscan.” In this respect, the Briançonnais basement therefore presents more similarities with the pre-Alpine basement of the Adriatic palaeomargin than with the European palaeomargin (i.e. the External Massifs).

Acknowledgments This work was financially supported by the Swiss National Science Foundation (project no.P300P2_147762) and by the AO-INSU 2013 Terre Solide program (CNRS). We would like to thank Matthias Bächli and Remo Widmer for their help in the mineral separation process. The “Ente Parco Nazionale Gran Paradiso” is thanked for allowing fieldwork and rock sampling in the Valnontey Valley. The “Villaggio Alpino Don Bosco” is thanked for the accommodation at the Alpe Money hut. We thank reviewers Marco Malusà and Ralph Schuster as well as the editor Wolf-Christian Dullo for their corrections and suggestions which have substantially improved the manuscript.

References

- Abrecht J, Biino GG, Schaltegger U (1995) Building the European continent: late Proterozoic–early Paleozoic accretion in the Central Alps of Switzerland. EUG 8, Strasbourg, Terra Abstracts 7/1:105
- Amstutz A (1962) Notice pour une carte géologique de la vallée de Cogne et de quelques autres espaces au sud d'Aoste. Arch Sci 15:1–104
- Arthaud F, Matte PH (1977) Late Palaeozoic strike-slip faulting in Southern Europe and Northern Africa. Geol Soc Am Bull 88:1305–1320
- Ballèvre M (1988) Collision continentale et chemins P-T: L'unité pennique du Grand Paradis (Alpes occidentales). Mém Géosci Rennes 19:340
- Battiston P, Benciolini L, Dal Piaz GV, De Vecchi G, Marchi G, Martin S, Polino R, Tartarotti P (1984) Geologia di una traversa dal

- Gran Paradiso alla zona Sesia-Lanzo in alta Val Soana, Piemonte. *Memorie della Società Geologica Italiana* 29:209–232
- Beltrando M, Rubatto D, Manatschal G (2010) From passive margins to orogens: the link between ocean-continent transition zones and (ultra)high-pressure metamorphism. *Geology* 38:559–562
- Bencolini L, Martin S, Tartarotti P (1984) Il metamorfismo eclogitico nel basamento del Gran Paradiso ed in unità piemontesi della valle di Campiglia. *Memorie della Società Geologica Italiana* 29:127–151
- Bertrand JM, Leterrier J (1997) Granitoïdes d'âge Paléozoïque inférieur dans le socle de Vanoise méridionale: géochronologie U-Pb du métagranite de l'Arpont (Alpes de Savoie, France). *Comptes Rendus de l'Académie des Sciences Paris II* 325:839–844
- Bertrand JM, Guillot F, Leterrier J, Perruchot M-P, Aillères L, Macaudière J (1998) Granitoïdes de la zone houillère briançonnaise en Savoie et en Val d'Aoste (Alpes occidentales): géologie et géochronologie U-Pb sur zircon. *Geodin Acta* 11:33–49
- Bertrand JM, Guillot F, Leterrier J (2000a) Age Paléozoïque inférieur (U-Pb sur zircon) de métagranophyres de la nappe du Grand-Saint-Bernard (zona interna, vallée d'Aoste, Italie). *Comptes Rendus de l'Académie des Sciences de Paris* 330:473–478
- Bertrand JM, Pidgeon RT, Leterrier J, Guillot F, Gasquet D, Gattiglio M (2000b) SHRIMP and IDTIMS U-Pb zircon ages of the pre-Alpine basement in the Internal Western Alps (Savoy and Piemont). *Schweiz Mineral Petrogr Mitt* 80:225–248
- Bertrand JM, Paquette J-L, Guillot F (2005) Permian zircon U-Pb ages in the Gran Paradiso massif: revisiting post-Variscan events in the Western Alps. *Schweiz Mineral Petrogr Mitt* 85:15–29
- Bonin B, Brändlein P, Bussy F, Eggenberger U, Finger F, Graf K, Marro C, Mercolli I, Oberhaensli R, Ploquin A, Von Quadt A, Von Raumer JF, Schaltegger U, Steyer HP, Visonà D, Vivier G (1993) Late Variscan magmatic evolution of the Alpine basement. In: von Raumer JF, Neubauer F (eds) Pre-Mesozoic geology in the Alps. Springer, Berlin, pp 171–201
- Boriani A, Sassi F, Sassi R (2003) The basement complexes in Italy, with special regards to those exposed in the Alps: a review. *Episodes* 26:186–192
- Brousmiche Delcambre C, Mercier D, Coquel R (1995) Implications stratigraphiques de la révision de la flore carbonifère au Sud de Briançon. *Comptes Rendus de l'Académie des Sciences Paris II* 320:335–340
- Brousmiche Delcambre C, Coquel R, Mercier D (1997) Sur l'âge des terrains carbonifères affleurant au col de Tramouillon (Massif de Gaulent, Sud Briançonnais). *Rev Paléobiol* 16:169–179
- Brousmiche Delcambre C, Coquel R, Decrouez D (1999) Sur la flore de deux gisements carbonifères de la Zone delphino-helvétique: carrière d'Héry-sur-Ugine (Vallée de l'Arly); Ardoisières des Posettes (Massif des Aiguilles Rouges)—Haute-Savoie (France). *Revue Paléobiol* 18:317–331
- Brouwer FM, Vissers RLM, Lamb WM (2002) Structure and metamorphism of the Gran Paradiso massif, western Alps, Italy. *Contrib Miner Petrol* 143:450–470
- Bussy F, Cadoppi P (1996) U-Pb zircon dating of granitoids from the Dora-Maira massif (western Italian Alps). *Schweiz Mineral Petrogr Mitt* 76:217–233
- Bussy F, von Raumer JF (1994) U-Pb geochronology of Palaeozoic magmatic events in the Mont-Blanc Crystalline Massif, Western Alps. *Schweiz Mineral Petrogr Mitt* 74:514–515
- Bussy F, Delitroz D, Fellay R, Hernandez J (1998a) The Pormenaz Monzonite (Aiguilles Rouges, Western Alps): an additional evidence for a 330 Ma-old magnesio-potassic magmatic suite in the Variscan. *Schweiz Mineral Petrogr Mitt* 78:193–194
- Bussy F, Venturini G, Hunziker JC, Martinotti G (1998b) U-Pb ages of magmatic rocks of the western Austroalpine Dent-Blanche-Sesia Unit. *Schweiz Mineral Petrogr Mitt* 78:163–168
- Bussy F, Hernandez J, von Raumer JF (2000a) Bimodal magmatism as a consequence of the post-collisional readjustment of the thickened Variscan continental lithosphere (Aiguilles Rouges—Mont Blanc Massifs, Western Alps). *Geol Soc Am Spec Papers* 350:221–233
- Bussy F, Hernandez J, von Raumer JF (2000b) Bimodal magmatism as a consequence of the post-collisional readjustment of the thickened variscan continental lithosphere (Aiguilles Rouges/Mont-Blanc massifs, western Alps). *Trans R Soc Edinb Earth Sci* 91:221–233
- Cadel G, Cosi M, Pennacchioni G, Spalla MI (1996) A new map of the Permo-Carboniferous cover and Variscan metamorphic basement in the central Orobic Alps, Southern Alps, Italy: structural and stratigraphical data. *Memorie di Scienze Geologiche* 48:1–53
- Capuzzo N, Bussy F (2000) High-precision dating and origin of syn-sedimentary volcanism in the Late Carboniferous Salvan-Dorénaz basin (Aiguilles-Rouges Massif, Western Alps). *Schweiz Mineral Petrogr Mitt* 80:147–167
- Capuzzo N, Wetzel A (2004) Facies and basin architecture of the Late Carboniferous Salvan-Dorénaz continental basin (Western Alps, Switzerland/France). *Sedimentology* 51:675–697
- Capuzzo N, Handler R, Neubauer F, Wetzel A (2003) Post-collisional rapid exhumation and erosion during continental sedimentation: the example of the late Variscan Salvan-Dorénaz basin (Western Alps). *Int J Earth Sci* 92:364–379
- Cassinis G, Doubinger J (1992) Artinskian and Ufimian palynomorph assemblages from the central Southern Alps, Italy, and their stratigraphic regional implications. Paper presented at the In: Nairn AEM, Korotev V (ed) Contribution to Eurasian geology. International congress on the Permian system of the world. Columbia University of South Carolina, Perm, Russia, pp 9–18
- Cassinis G, Perotti CR (2007) A stratigraphic and tectonic review of the Italian Southern Alpine Permian. *Palaeoworld* 16:140–172
- Cassinis G, Massari F, Neri C, Venturini C (1988) The continental Permian of the Southern Alps. A review. *Zeitschrift für Geologische Wissenschaften* 16:117–126
- Cassinis G, Nadège T-M, Carmina V (1995) A general outline of the Permian continental basins in Southwestern Europe. In: Scholle PA, Peryt TM (eds) Ulmer-Scholle DS: the permian of Northern Pangea. Springer, New York, pp 137–157
- Cassinis G, Nicosia U, Pittau P, Ronchi A (2002) Palaeontological and radiometric data from the Permian continental deposits of the Central-Eastern Southern Alps (Italy), and their stratigraphic implications. *Mémoire de l'Association des Géologues du Permien* 2:53–74
- Cassinis G, Perotti CR, Ronchi A (2012) Permian continental basins in the Southern Alps (Italy) and peri-mediterranean correlations. *Int J Earth Sci* 101:129–157
- Cenki-Tok B, Oliot E, Rubatto D, Berger A, Engi M, Janots E, Thomsen TB, Manzotti P, Regis D, Spandler C, Robyr M, Goncalves P (2011) Preservation of Permian allanite within an Alpine eclogite facies shear zone at Mt Mucrone, Italy: mechanical and chemical behavior of allanite during mylonitization. *Lithos* 125:40–50
- Compagnoni R, Lombardo B (1974) The Alpine age of the Gran Paradiso eclogites. *Rendiconti della Società Italiana di Mineralogia e Petrologia* 30:220–237
- Compagnoni R, Prato R (1969) Paramorfosi di cianite su sillimanite in scisti pregranitici del massiccio del Gran Paradiso. *Bollettino della Società Geologica Italiana* 88:537–549
- Compagnoni R, Elter G, Lombardo B (1974) Eterogeneità stratigrafica del complesso degli “gneiss minimi” nel massiccio del Gran Paradiso. *Memorie della Società Geologica Italiana* 13:227–239

- Corfu F, Hanchar JM, Hoskin PWO, Kinny P (2003) Atlas of zircon textures. *Rev Mineral Geochem* 53:469–500
- Corsin P, Faure-Muret A (1946) Découverte d'une florule stéphanienne au Cirque de Férisson près de Saint-Martin-Vésubie (A.-M.). *Compte-Rendu des Séances de la Société Géologique de France*, pp 246–247
- Cortesogno L, Cassinis G, Dallagiovanna G, Gaggero L, Oggiano G, Ronchi A, Seno S, Vanossi M (1998) The Variscan post-collisional volcanism in Late Carboniferous-Permian sequences of Ligurian Alps, Southern Alps and Sardinia (Italy): a synthesis. *Lithos* 45:305–328
- Dal Cin R (1972) I conglomerati tardo-paleozoici post-ercinici delle Dolomiti. *Mitteilungen der Gesellschaft der Geologie und Bergbaustudenten in Österreich* 20:47–74
- Dal Piaz GV, Lombardo B (1986) Early Alpine eclogite metamorphism in the Penninic Monte Rosa-Gran Paradiso basement of the northwestern Alps. In: Evans BW, Brown EH (ed) Blueschists and Eclogites, Memoir, Geological Society of America, vol 164, pp 249–265
- Darby BJ, Gehrels GE (2006) Detrital zircon reference for the North China block. *J Asian Earth Sci* 26:637–648
- Decelles PG, Gehrels GE, Najman Y, Martin AJ, Carter A, Garzanti E (2004) Detrital geochronology and geochemistry of Cretaceous-Early Miocene strata of Nepal: implications for timing and diachroneity of initial Himalayan orogenesis. *Earth Planet Sci Lett* 227:313–330
- Diella V, Spalla MI, Tunesi A (1992) Contrasting thermomechanical evolutions in the southalpine metamorphic basement of the orobic alps (Central Alps, Italy). *J Metamorph Geol* 10:203–219
- Ducassou C, Poujol M, Ruffet G, Bruguier O, Ballèvre M (2014) Relief variations and erosion of the Variscan belt: detrital geochronology of the Palaeozoic sediments from the Mauges Unit (Armorican Massif, France). *Geol Soc Lond Spec Publ* 405:137–167
- Ellenberger F (1958) Étude géologique du pays de Vanoise (Savoie). *Mémoires du Service de la Carte Géologique de la France*, p 464
- Ellenberger F (1966) Le Permien du pays de Vanoise—Atti del symposium sul Verrucano, Pisa, 1965. *Società Toscana di Scienze Naturali*, pp 170–211
- Elter G (1960) La zona pennidica dell'alta e media Valle d'Aosta e le unità limítrofe. *Memorie degli Istituti di Geologia e Mineralogia dell'Università di Padova* 23:160
- Elter G (1972) Contribution à la connaissance du Briançonnais interne et de la bordure piémontaise dans les Alpes grises nord-orientales et considérations sur le rapports entre les zones du Briançonnais et des Schistes Lustrés. *Memorie degli Istituti di Geologia e Mineralogia dell'Università di Padova* 28:19
- Ewing TA, Hermann J, Rubatto D (2013) The robustness of the Zr-in-rutile and Ti-in-zircon thermometers during high-temperature metamorphism (Ivrea-Verbano Zone, northern Italy). *Contrib Miner Petrol* 165:757–779
- Fabre J (1961) Contribution à l'étude de la Zone Houillière en Maurienne en Tarentaise. *Mémoires du Bureau de Recherches Géologiques et Minières* 2:315
- Fabre R, Gidon M, Tricart P (1982) La structure du Paléozoïque de la Zone briançonnaise axiale au Nord de Névache. *Géologie Alpine* 58:31–52
- Faure G, Mensing TM (2005) Isotopes: principles and applications. Wiley, Hoboken, p 897
- Faure-Muret A (1955) Études géologiques sur le massif de l'Argentera-Mercantour. *Mémoires du Service de la Carte Géologique de la France*, p 336
- Fedo CM, Sircombe KN, Rainbird RH (2003) Detrital zircon analysis of the sedimentary record. In: Hanchar, JM, Hoskin, PWO (eds) Zircon reviews in mineralogy and geochemistry, mineralogical society of America, vol 53, pp 277–303
- Feys R (1963) Etude géologique du carbonifère Briançonnais. *Mémoires du Bureau de Recherches Géologiques et Minières* 6:387
- Finger F, Roberts MP, Haunschmid B, Schermaier A, Steyer HP (1997) Variscan granitoids of central Europe: their typology, potential sources and tectonothermal relations. *Mineral Petrol* 61:67–96
- Fluteau F, Besse J, Broutin J, Ramstein G (2001) The late Permian climate. what can be inferred from climate modeling concerning Pangaea scenarios and Hercynian range altitude. *Palaeogeogr Palaeoclimatol Palaeoecol* 167:39–71
- Franz L, Romer RL (2007) Caledonian high-pressure metamorphism in the Strona-Ceneri Zone (Southern Alps of southern Switzerland and northern Italy). *Swiss J Geosci* 100:457–467
- Franz G, Mosbrugger V, Menge R (1991) Carbo-Permian pteridophyll leaf fragments from an amphibolite facies basement, Tauern Window, Austria. *Terra Nova* 3:137–141
- Gabudianu Radulescu I, Compagnoni R, Lombardo B (2011) Poly-metamorphic history of a relict Permian hornfels from the central Gran Paradiso Massif (Western Alps, Italy): a microstructural and thermodynamic modelling study. *J Metamorph Geol* 29:851–874
- Gaggero L, Cortesogno L, Bertrand JM (2004) The pre-Namurian basement of the Ligurian Alps: a review of the lithostratigraphy, pre-Alpine metamorphic evolution, and regional comparisons. *Periodico di Mineralogia* 73:85–96
- Gasco I, Borghi A, Gattiglio M (2010) Metamorphic evolution of the Gran Paradiso Massif: a case study of an eclogitic metagabbro and a polymetamorphic glaucophane-garnet micaschist. *Lithos* 115:101–120
- Gebauer D, Quadt A, Compston W, Williams IS, Grünenfelder M (1988) Archaean zircons in a retrograded, Caledonian eclogite of the Gotthard Massif (Central Alps, Switzerland). *Schweiz Mineral Petrogr Mitt* 68:485–490
- Gignoux M, Moret L (1952) Géologie Dauphinoise. Initiation à la géologie par l'étude des environs de Grenoble. Masson et Cie, Paris, p 391
- Greber C (1965) Flore et stratigraphie du Carbonifère des Alpes françaises. *Mémoires du Bureau de Recherches Géologiques et Minières* 21:380
- Gretter N, Ronchi A, Langone A, Perotti CR (2013) The transition between the two major Permian tectono-stratigraphic cycles in the Southern Alps: results from facies analysis and U/Pb geochronology. *Int J Earth Sci* 102:1181–1202
- Guerrot C, Debon F (2000) U-Pb zircon dating of two contrasting Late Variscan plutonic suites from the Pelvoux massif (French Western Alps). *Schweiz Mineral Petrogr Mitt* 80:249–256
- Guillot F, Liégeois J-P, Fabre J (1991) Late Cambrian Mt Pourri granophyres, first dating by U-Pb on zircon of a basement in the internal French Alps (Penninic Alps, Briançonnais Zone, Vanoise). *Comptes Rendus de l'Académie des Sciences Paris II* 313:239–244
- Guillot F, Schaltegger U, Bertrand JM, Deloule E, Baudin T (2002) Zircon U-Pb geochronology of Ordovician magmatism in the polycyclic Ruitor Massif (Internal W-Alps). *Int J Earth Sci* 91:964–978
- Guimara M (1989) Le Carbonifère des chaînes subalpines de haute Provence (France) dans son cadre structural. PhD dissertation, Université de Provence (Aix-Marseille I), p 128
- Gutiérrez-Alonso G, Fernández-Suárez J, Weil AB, Murphy JB, Nance RD, Corfu F, Johnston ST (2008) Self-subduction of the Pangean global plate. *Nat Geosci* 1:540–553
- Haudour J (1976) Les Hoillères du Dauphiné. Le gisement d'anthracite de La Mure. *Industrie minérale* 58:65–75
- Heaman LM, Bowins R, Crocket J (1990) The chemical composition of igneous zircon suites: implications for geochemical tracer studies. *Geochim Cosmochim Acta* 54:1597–1607

- Hermann J, Rubatto D (2003) Relating zircon and monazite domains to garnet growth zones: age and duration of granulite facies metamorphism in the Val Malenco lower crust. *J Metamorph Geol* 21:833–852
- Hietpas J, Samson S, Moecher D, Chakraborty S (2011) Enhancing tectonic and provenance information from detrital zircons studies: assessing terrane-scale sampling and grain-scale characterization. *J Geol Soc Lond* 168:309–318
- Hoinkes G, Thöni M (1993) Evolution of the Ötztal-Stubai, Scarl-Campo and Ulten basement units. In: von Raumer JF, Neubauer F (eds) Pre-Mesozoic geology in the Alps. Springer, Berlin, pp 485–494
- Jackson SE, Pearson NJ, Griffin WL, Belousova EA (2004) The application of laser-ablation-inductively coupled plasma-mass spectrometry to in situ U-Pb zircon geochronology. *Chem Geol* 211:47–69
- Jongmans W (1960) Die Karbongflora der Schweiz. Mit einem Beitrag von Ritter, E.: Die Karbon-Vorkommen der Schweiz. Beiträge zur geologischen Karte der Schweiz 108:1–95
- Kebede T, Klötzli U, Kosler J, Skiold T (2005) Understanding the pre-Variscan and Bariscan basement components of the central Tauern Window, Eastern alps (Austria): constraints from zircon U-Pb geochronology. *Int J Earth Sci* 94:336–353
- Klötzli-Chowanetz E, Klötzli U, Koller F (1997) Lower Ordovician migmatisation in the Ötztal crystalline basement (Eastern Alps, Austria): linking U-Pb and Pb-Pb dating with zircon morphology. *Schweiz Mineral Petrogr Mitt* 77:315–324
- Königer S, Lorenz V, Stollhofen H, Armstrong RA (2002) Origin, age and stratigraphic significance of distal fallout ash tuffs from the Carboniferous-Permian continental Saar-Nahe basin (SW Germany). *Int J Earth Sci* 91:341–356
- Köppel V, Grünenfelder M (1971) A study of inherited and newly formed zircons from paragneisses and granitised sediments of the Strona-Ceneri-Zone (Southern Alps). *Schweiz Mineral Petrogr Mitt* 51:385–409
- Krainer K (1993) Late and post-Variscan sediments of the Eastern and Southern Alps. In: von Raumer JF, Neubauer F (eds) Pre-Mesozoic geology in the Alps. Springer, Berlin, pp 564–573
- Kutzbach JE, Ziegler AM (1993) Simulation of the Late Permian climate and biomes with an atmosphere-ocean model: comparisons with observations. *Philos Trans R Soc Lond B* 341:327–340
- Kydonakis K, Kostopoulos D, Poujol M, Brun J-P, Papanikolau D, Paquette J-L (2014) The dispersal of the Gondwana Super-fan System in the eastern Mediterranean: new insights from detrital zircon geochronology. *Gondwana Res* 25:1230–1241
- Lahtinen R, Huhma H, Kousa J (2002) Contrasting source components of the Paleoproterozoic Svecfennian metasediments: detrital zircon U-Pb, Sm-Nd and geochemical data. *Precambr Res* 116:81–109
- Lardeaux JM, Spalla MI (1991) From granulites to eclogites in the Sesia zone (Italian Western Alps): a record of the opening and closure of the Piedmont ocean. *J Metamorph Geol* 9:35–59
- Le Bayon B, Ballèvre M (2004) Field and petrological evidence for a Late Palaeozoic (Upper Carboniferous-Permian) age of the Erfaufer orthogneiss (Gran Paradiso, western Alps). *CR Geosci* 336:1079–1089
- Le Bayon B, Ballèvre M (2006) Deformation history of a subducted continental crust (Gran Paradiso, Western Alps): continuing crustal shortening during exhumation. *J Struct Geol* 28:793–815
- Le Bayon B, Pitra P, Ballèvre M, Bohn M (2006) Reconstructing P-T paths during continental collision using multi-stage garnet (Gran Paradiso nappe, Western Alps). *J Metamorph Geol* 24:477–496
- Le Goff E, Ballèvre M (1990) Geothermobarometry in albite-garnet orthogneisses: a case study from the Gran Paradiso nappe (Western Alps). *Lithos* 25:261–280
- Linnemann U, Ouzegane K, Drareni A, Hofmann M, Becker S, Gärtner A, Sagawe A (2011) Sands of West Gondwana: an archive of secular magmatism and plate interactions—a case study from the Cambro-Ordovician section of the Tassili Ouan Ahaggar (Algerian Sahara) using U-Pb-LA-ICP-MS detrital zircon ages. *Lithos* 123:188–203
- Ludwig KR (2003) Isoplot/Ex version 3.0. A geochronological toolkit for Microsoft Excel. Geochronological Centre Special Publication, Berkeley, p 70
- Malusà MG, Villa IM, Vezzoli G, Garzanti E (2011) Detrital geochronology of unroofing magmatic complexes and the slow erosion of Oligocene volcanoes in the Alps. *Earth Planet Sci Lett* 301:324–336
- Malusà MG, Carter A, Limoncelli M, Villa IM, Garzanti E (2013) Bias in detrital zircon geochronology and thermochronometry. *Chem Geol* 359:90–107
- Manzotti P, Ballèvre M (2013) Multistage garnet in high-pressure metasediments: alpine overgrowths on Variscan detrital grains. *Geology* 41:1151–1154
- Manzotti P, Rubatto D, Darling J, Zucali M, Cenki-Tok B, Engi M (2012) From Permo-Triassic lithospheric thinning to Jurassic rifting at the Adriatic margin: petrological and geochronological record in Valtournenche (Western Italian Alps). *Lithos* 146–147:276–292
- Manzotti P, Carlier Le, de Veslud C, Le Bayon B, Ballèvre M (2014) Petro-structural map of the Money Unit (Gran Paradiso Massif, Valnontey valley, Western Alps). *J Maps* 10:324–340
- Marotta AM, Spalla MI (2007) Permian-Triassic high thermal regime in the Alps: Result of late Variscan collapse or continental rifting? Validation by numerical modeling. *Tectonics* 26(4). doi:10.1029/2006TC002047
- Massari F (1988) Some thoughts on the Permo-Triassic evolution of the South-Alpine area. *Memorie della Società Geologica Italiana* 34:179–188
- Massari F, Neri C, Pittau P, Fontana D, Stefani C (1994) Sedimentology, palynostratigraphy and sequence stratigraphy of a continental to shallow-marine rift-related succession: upper Permian of the eastern Southern Alps (Italy). *Memorie di Scienze Geologiche, Padova* 46:119–243
- Matte P (1986) Tectonics and plate tectonics model for the Variscan belt of Europe. *Tectonophysics* 126:329–374
- McCann T, Skompski S, Poty E, Dusar M, Vozárová K, Schneider J, Wetzel A, Krainer K, Kornpahl K, Schäfer M, Krings M, Oplustil S, Tait J (2008) Carboniferous. In: McCann T (Ed) The geology of Central Europe, the geological society, vol 9, pp 411–529
- Ménard G, Molnar P (1988) Collapse of a Hercynian tibetan Plateau into a late Palaeozoic European Basin and Range province. *Nature* 334:235–237
- Ménot R-P, Peucat JJ, Scarenzi D, Piboule M (1988) 496 My age of plagiogranites in the Chamrousse ophiolite complex (external crystalline massifs in the French Alps): evidence of a Lower Paleozoic oceanization. *Earth Planet Sci Lett* 88:82–92
- Mercier D, Beaudoin B (1984) Le Briançonnais au Carbonifère: modalités de la subsidence d'une gouttière méridienne. *Comptes Rendus de l'Académie des Sciences de Paris* 298:125–128
- Mercier D, Beaudoin B (1987) Révision du Carbonifère Briançonnais: stratigraphie et évolution du bassin. *Géologie Alpine Mémoires* 13:25–31
- Miller C, Thöni M (1997) Eo-Alpine eclogitisation of Permian MORB-type gabbros in the Koralpe (Eastern Alps, Austria): new geochronological, geochemical and petrological data. *Chem Geol* 137:283–310
- Monjoie P, Bussy F, Lapierre H, Pfeifer HR (2005) Modeling of in situ crystallization processes in the Permian mafic layered

- intrusion of Mont Collon (Dent Blanche nappe, western Alps). *Lithos* 83:317–346
- Müntener O, Hermann J (2001) The role of lower crust and continental upper mantle during formation of non-volcanic passive margins: evidence from the Alps. *Geol Soc Lond Spec Publ* 187:267–288
- Nemchin AA, Canwood PA (2005) Discordance of the U-Pb system in detrital zircons: implication for provenance studies of sedimentary rocks. *Sed Geol* 182:143–162
- Neubauer F, Sassi FP (1993) The Austro-Alpine quartzphyllites and rekkated Paleozoic formations. In: von Raumer JF, Neubauer F (eds) Pre-Mesozoic geology in the Alps. Springer, Berlin, pp 423–439
- Nicosia U, Ronchi A, Santi G (2000) Permian tetrapod footprints from W Orobic Basin (Northern Italy). Biochronological and evolutionary remarks. *Geobios* 33:753–768
- Niklaus P-A, Wetzel A (1996) Faziesanalyse und Ablagerungsmilieu der fluviatilen Sedimenttüfflung des Karbontriges von Salvano-Dorénaz. *Eclogae Geol Helv* 89:427–437
- Novarese V (1894) Dioriti granitoidi e gneissiche della Valsavarenche (Alpi Graie). *Bollettino del Regio Comitato geologico d'Italia XXV*:275–300
- Novarese V (1895) Rilevamento geologico eseguito nel 1894 in valle della Germanasca (Alpi Cozie). *Bollettino del Regio Comitato geologico d'Italia XXVI*:253–282
- Novarese V (1896) Sul rilevamento geologico del 1895 nella val Pellice (Alpi Cozie). *Bollettino del Regio Comitato geologico d'Italia XXVII*:231–267
- Oberli F, Sommerauer J, Steiger RH (1981) U-(Th)-Pb systematics and mineralogy of single crystals and concentrates from the Cacciola granite, central Gotthard massif, Switzerland. *Schweiz Mineral Petrogr Mitt* 61:323–348
- Oberli F, Meier M, Biino GG (1994) Time constraints on the pre-Vari-scan magmatism/metamorphic evolution of the Gotthard and Tavetsch units derived from single crystal U-Pb results. *Schweiz Mineral Petrogr Mitt* 74:483–488
- Opluštík S, Šimunek Z, Zajíč J, Mencl V (2013) Climatic and biotic changes around the Carboniferous/Permian boundary recorded in the continental basins of the Czech Republic. *Int J Coal Geol* 119:114–151
- Peressini G, Quick JE, Sinigoi S, Hofmann AW, Fanning M (2007) Duration of a large Mafic intrusion and heat transfer in the lower crust: a SHRIMP U-Pb zircon study in the Ivrea-Verbano Zone (Western Alps, Italy). *J Petrol* 48:1185–1218
- Pestal G, Brueggemann-Ledolter M, Draxler I, Eibinger D, Eichberger H, Reooter C, Scevik F, Fritz A, Koller F (1999) Ein Vorkommen von Oberkarbon in den mittleren Hohen Tauern. *Jahrbuch der Geologischen Bundesanstalt Wien* 141:491–502
- Pognante U (1980) Preliminary data on the Piemonte ophiolite nappe in the lower Val Susa-Val Chisone area, Western Alps. *Ofioliti* 5:221–240
- Polino R, Dal Piaz GV (1978) Geologia dell'alta Val d'Isère e del bacino del Lago Serrù (Alpi Graie). *Memorie degli Istituti di Geologia e Mineralogia dell'Università di Padova* 32:1–19
- Portis A (1887) Sulla scoperta delle piante fossili carbonifere di Viozene nell'alta valle del Tanaro. *Bollettino del Regio Comitato geologico d'Italia* 18:417–420
- Powers MC (1953) A new roundness scale for sedimentary particles. *J Sediment Petrol* 23:117–119
- Quick JE, Sinigoi S, Peressini G, Demarchi G, Wooden JL, Sbisà A (2009) Magmatic plumbing of a large Permian caldera exposed to a depth of 25 km. *Geology* 37:603–606
- Raumer JF, Bussy R, Schaltegger U, Schulz B, Stampfli GM (2012) Pre-Mesozoic Alpine basements—their place in the European Paleozoic framework. *Geol Soc Am Bull* 125:89–108
- Ring U, Collins AS, Kassem OK (2005) U-Pb SHRIMP data on the crystallization age of the Gran Paradiso augengneiss, Italian Western Alps: further evidence for Permian magmatic activity in the Alps during break-up of Pangea. *Eclogae Geol Helv* 98:363–370
- Ronchi A, Kustatscher R, Pittau P, Santi G (2012) Pennsylvania floras from Italy: an overview of the main sites and historical collections. *Geol Croat* 65:299–322
- Roscher M, Schneider JW (2006) Permo-Carboniferous climate: early Pennsylvanian to Late Permian climate development of central Europe in a regional and global context. In: Lucas SG, Cassinis G, Schneider JW (ed) Non-Marine Permian Biostratigraphy and biochronology. The Geological Society of London, special publications, vol 265, pp 95–136
- Rubatto D (2002) Zircon trace element geochemistry: partitioning with garnet and the link between U-Pb ages and metamorphism. *Chem Geol* 184:123–138
- Rubatto D, Gebauer D (1997) The Bonze Unit (Sesia-Lanzo Zone, Western Alps): a gabbroic Early Carboniferous intrusion that recorded Hecynian and Alpine metamorphism. *Quaderni di Geodinamica Alpina e Quaternaria* 4:106–107
- Rubatto D, Gebauer D (2000) Use of cathodoluminescence for U-Pb zircon dating by ion microprobe: some examples from the Western Alps. In: Pagel M, Barbin V, Blanc P, Ohnenstetter D (eds) Cathodoluminescence in geosciences, vol 15. Springer, Heidelberg, pp 373–400
- Rubatto D, Hermann J (2001) Exhumation as fast as subduction? *Geology* 29:3–6
- Rubatto D, Gebauer D, Compagnoni R (1999) Dating of eclogite facies zircons: the age of Alpine metamorphism in the Sesia-Lanzo Zone (Western Alps). *Earth Planet Sci Lett* 167:141–158
- Rubatto D, Schaltegger U, Lombardo B, Colombo F, Compagnoni R (2001) Complex paleozoic magmatic and metamorphic evolution in the Argentera Massif (Western Alps) resolved with U-Pb dating. *Schweiz Mineral Petrogr Mitt* 81:213–228
- Schade J, Greber C, Fabre J (1985) Nouvelles récoltes de plantes dans la zone houillère (Alpes françaises) au col de la Ponsonnière (Valloire) et au mont du Vallon (Méribel). *Géologie Alpine* 61:165–172
- Schaltegger U, Brack P (2007) Crustal scale magmatic system during intracontinental strike-slip tectonics: U, Pb and Hf isotopic constraints for Permian magmatic rocks of the Southern Alps. *Int J Earth Sci* 96:1131–1151
- Schaltegger U, Corfu F (1992) The age and source of late Hercynian magmatism in the central Alps: evidence from precise U-Pb ages and initial Hf isotopes. *Contrib Miner Petrol* 111:329–344
- Schaltegger U, Corfu F (1995) Late Variscan “Basin and Range” magmatism and tectonics in the Central Alps: evidence from U-Pb geochronology. *Geodin Acta* 8:82–98
- Schaltegger U, von Quadt A (1990) U-Pb zircon dating of the Central Aar granite (Aar Massif, Switzerland). *Schweiz Mineral Petrogr Mitt* 70:361–371
- Schaltegger U, Fanning CM, Günther D, Maurin JC, Schulmann K, Gebauer D (1999) Growth annealing and recrystallization of zircon and preservation of monazite in high-grade metamorphism: conventional and in situ U-Pb isotope, cathodoluminescence and microchemical evidence. *Contrib Miner Petrol* 134:186–201
- Schaltegger U, Gebauer D, von Quadt A (2002) The mafic-ultramafic rock association of Loderio-Biasca (lower Pennine nappes, Ticino, Switzerland): Cambrian oceanic magmatism and its bearing on early Paleozoic paleogeography. *Chem Geol* 186:265–279
- Scheiber T, Berndt J, Heredia BD, Mezger K, Pfiffner A (2013) Episodic and long-lasting Paleozoic felsic magmatism in the

- pre-Alpine basement of the Suretta nappe (eastern Swiss Alps). *Int J Earth Sci* 102:2097–2115
- Scheiber T, Berndt J, Mezger K, Pfiffner A (2014) Precambrian to Paleozoic zircon record in the Siviez-Mischabel basement (western Swiss Alps). *Swiss J Geosci* 107:49–64
- Schmid SM, Fügenschuh B, Kissling E, Schuster R (2004) Tectonic map and overall architecture of the Alpine orogen. *Eclogae Geol Helv* 97:93–117
- Schneider JW, Körner F, Roscher M, Kröner U (2006) Permian climate development in the northern Peri-Tethys area: the Lodève Basin, French Massif Central, compared in a European and global context. *Palaeogeogr Palaeoclimatol Palaeoecol* 240:161–183
- Schönlau HP (1992) Stratigraphy, biogeography and paleoclimatology of the Alpine Paleozoic and its implications for plate movements. *Jahrbuch Geologische Bundesanstalt Wien* 135:381–418
- Schönlau HP (1993) Stratigraphy, biogeography and climatic relationships of the Alpine Paleozoic. In: von Raumer JF, Neu- bauer F (eds) Pre-Mesozoic geology in the Alps. Springer, Berlin, pp 65–91
- Schuster R, Stüwe K (2008) Permian metamorphic event in the Alps. *Geology* 36:603–606
- Schuster R, Scharbert S, Abart R, Frank W (2001) Permo-Triassic extension and related HT/LP metamorphism in the Austroalpine—Southalpine realm. *Mitteilungen der Gesellschaft der Geologie und Bergbaustudenten in Österreich* 45:111–141
- Sergeev SA, Steiger RH (1993) High-precision U-Pb single zircon dating of Variscan and Caledonian magmatic cycles in the Gotthard Massif, Central Alps. *Terra Abstracts* 5:394–395
- Servais T, Dzik J, Fatka O, Heuse T, Vecoli M, Verniers J (2008) Ordovician. In: McCann T (ed) The geology of Central Europe, the geological society, vol 5, pp 203–248
- Sláma J, Košler J (2012) Effects of sampling and mineral separation on accuracy of detrital zircon studies. *Geochem Geophys Geosyst* 13:Q05007
- Smirnov NV (1939) On the estimation of the discrepancy between empirical curves of distribution for two independent samples. *Mosc Univ Math Bull* 2:3–14
- Spalla MI, Zanoni D, Marotta AM, Gisella R, Roda M, Zucali M, Gosso G (2014) The transition from Variscan collision to continental break-up in the Alps: advices from the comparison between natural data and numerical model predictions. *Geol Soc Lond Spec Pub* 405:363–400
- Steiger RH, Meier M, Iizumil S, Bickel RA (1994) The polyorogenic nature of the Simano nappe as derived from single-zircon U/Pb data. *Schweiz Mineral Petrogr Mitt* 74:526–527
- Talavera C, Montero P, Martínez Poyatos D, Williams IS (2012) Ediacaran to Lower Ordovician age for rocks ascribed to the Schist-Graywacke Complex (Iberian Massif, Spain): evidence from detrital zircon SHRIMP U-Pb geochronology. *Gondwana Res* 22:928–942
- Teipel U, Eichhorn R, Loth G, Rohrmüller J, Höll R, Kennedy A (2004) U-Pb SHRIMP and Nd isotopic data from the western Bohemian Massif (Bayerischer Wald, Germany): implications for Upper Vendian and Lower Ordovician magmatism. *Int J Earth Sci* 93:782–801
- Thern ER, Nelson DR (2012) Detrital zircon age structure within ca. 3 Ga metasedimentary rocks, Yilgarn Craton: elucidation of Hadean source terranes by principal component analysis. *Precambr Res* 214–215:28–43
- Thöni M, Jagoutz E (1992) Some new aspect of dating eclogites in orogenic belts: Sm-Nd, Rb-Sr, and Pb-Pb isotopic results from the Austroalpine Saualpe and Koralpe type-locality (Karinthia/Styria, southeastern Austria). *Geochim Cosmochim Acta* 56:347–368
- Thöni M, Mottana A, Delitala MC, De Capitani L, Liborio G (1992) The Val Biandino composite pluton: a late Hercynian intrusion into the Southalpine metamorphic basement of the Alps (Italy). *Neues Jahrbuch für Mineralogie Monatshefte* 12:545–554
- Van Achterbergh E, Ryan CG, Jackson SE, Griffin WL (2001) Data reduction software for LA-ICP-MS: appendix. In: Sylvester PJ (Ed), *Laser Ablation-ICP-mass spectrometry in the Earth Sciences: principles and applications*, Mineralog Assoc Canada (MAC) Short Courses Series, Ottawa, Ontario, Canada, vol 29, pp 239–243
- Vavra G, Schmid R, Gebauer D (1999) Internal morphology, habit and U-Th-Pb microanalysis of amphibolite-to-granulite facies zircons: geochronology of the Ivrea Zone (Southern Alps). *Contrib Miner Petrol* 134:380–404
- Venzo S, Maglia L (1947) Lembali carboniferi trasgressivi sui micasisti alla “fronte sedimentaria sudalpina” del Comasco (Acquaserrata di Menaggio—Bocchetta di S. Bernardo) e del Varesotto (Bedero). *Atti della Società Italiana di Scienze Naturali* 86:33–70
- Vermeesch P (2012) On the visualisation of detrital age distributions. *Chem Geol* 312–313:190–194
- Vermeesch P (2013) Multi-sample comparison of detrital age distributions. *Chem Geol* 341:140–146
- Verniers J, Maletz J, Kříž J, Žigátková Ž, Paris F, Schönlau HP, Wrona R (2008) Silurian. In: McCann T (ed) The geology of Central Europe. Special Publication of the Geological Society, London, pp 249–302
- Veselà P, Lammerer B (2008) The Pfitsch-Mörchner Basin, an example of the post-Variscan sedimentary evolution in the Tauern Window (Eastern Alps). *Swiss J Geosci* 101(S1):73–88
- Vialon P (1966) Etude géologique du massif cristallin Dora-Maira (Alpes cottiennes internes, Italie). *Travaux du Laboratoire de Géologie de Grenoble* 4:293
- Vidal O, Parra T, Trotet F (2001) A thermodynamic model for Fe-Mg aluminous chlorite using data from the equilibrium experiments and natural pelitic assemblages in the 100° to 600°C, 1 to 25 kb range. *Am J Sci* 301:557–592
- Visonà D (1995) Polybaric evolution of calc-alkaline magmas: the dioritic belt of Bressanone-Chiusa igneous complex (NE Italy). *Memorie di Scienze Geologiche* 47:111–124
- Visonà D (1997) The Predazzo multipulse intrusive body (Western Dolomites, Italy): field and mineralogical studies. *Memorie di Scienze Geologiche* 49:117–125
- von Raumer JF (1993) Late Pre-Cambrian and Palaeozoic evolution of the Alpine Basement, an overview. In: von Raumer JF, Neu- bauer F (eds) Pre-Mesozoic geology in the Alps. Springer, Berlin, pp 625–640
- von Raumer JF (1998) The Paleozoic evolution of the Alps: from Gondwana to Pangea. *Geol Rundsch* 87:407–435
- von Raumer JF (2013) Pre-Mesozoic Alpine basements—their place in the European Paleozoic framework. *Geol Soc Am Bull* 125:89–108
- Vonlanthen P, Fitz Gerald JD, Rubatto D, Hermann J (2012) Recrys- tallization rims in zircon (Valle d’Arbedo, Switzerland): an integrated cathodoluminescence, LA-ICP-MS, SHRIMP, and TEM study. *Am Mineral* 97:369–377
- Wei CJ, Powell R, Zhang LF (2003) Eclogites from the south Tian- shan, NW China: petrological characteristic and calculated mineral equilibria in the Na₂O–CaO–FeO–MgO–Al₂O₃–SiO₂–H₂O system. *J Metamorph Geol* 21:163–179
- Wiedenbeck M, Allé P, Corfu F, Griffin WL, Meier M, Oberli F, von Quadt A, Roddick JC, Spiegel W (1995) Three natural zircon standards for U-Th-Pb, Lu-Hf, trace element and REE analyses. *Geostand Newslett* 19:1–23
- Wiedenbeck M, Hanchar JM, Peck WH, Sylvester P, Valley J, Whitehouse M, Kronz A, Morishita Y, Nasdala L, Fiebig J, Franchi I, Girard JP, Greenwood RC, Hinton R, Kita N, Mason PRD, Norman M, Ogasawara M, Piccoli PM, Rhede D, Satoh H, Schulz-Dobrick B,

- Skår Ø, Spicuzza MJ, Terada K, Tindle K, Togashi S, Vennemann T, Xie Q, Zheng YF (2004) Further characterisation of the 91500 zircon crystal. *Geostand Geoanal Res* 28:9–39
- Young IT (1977) Proof without prejudice: use of the Kolmogorov-Smirnov test for the analysis of histograms from flow systems and other sources. *J Histochem Cytochem* 25:935–941
- Ziegler PA (1993) Late Palaeozoic-Early Mesozoic plate reorganization: evolution and demise of the Variscan fold belt. In: von Raumer JF, Neubauer F (eds) Pre-Mesozoic geology in the Alps. Springer, Berlin, pp 203–216